Chapter 1

The seismic velocity structure of the deep continental crust

W. STEVEN HOLBROOK, WALTER D. MOONEY and NIKOLAS I. CHRISTENSEN

1. Introduction

Despite its importance to the study of continental crustal evolution, the composition of the lower part of the Earth's crust remains poorly known, largely because of the difficulty of directly sampling significant portions of it. Samples of lower-crustal rocks, which can be obtained from either xenoliths or high-grade metamorphic terrains, provide invaluable information on the composition of the deep crust, but it is difficult to assess their applicability to the lower crust as a whole. Geophysical techniques, however, provide a means of indirectly measuring physical properties across large sections of *in situ* lower crust. The physical properties determined by geophysical field experiments can then be compared to those measured in the laboratory on lower-crustal rock types, thereby placing constraints on the composition of the deep crust. One such physical property, which can be measured with seismological techniques, is seismic velocity.

We can infer the seismic velocity structure of the lower continental crust in two ways: either through seismic experiments on the Earth's surface, in which the velocity of seismic waves propagating through the lower crust is determined, or by measuring the speed of sound in laboratory specimens of rocks believed to have once resided in the lower crust. Each of these methods has advantages and drawbacks: seismic reflection/refraction studies provide information on the geometry and velocity structure of the *in situ* lower crust, but they are relatively expensive, and their resolution is limited by the wavelengths used (0.2–1.0 km). Laboratory studies, on the other hand, allow precise, relatively inexpensive measurements of physical properties, but the extrapolation of these properties to the scale of the *in situ* lower crust is uncertain. Naturally, field and laboratory studies are most effective when combined.

In this paper we summarize the current knowledge of the seismic velocity structure of the lower continental crust, as determined from both field seismic experiments and laboratory measurements. We restrict our summary of field results to wide-angle (refraction) seismic data: although narrow-aperture (reflection) seismology has in recent years produced many exciting insights into the structure of the lower crust, only wide-angle data provide accurate deep velocity information. For reviews of recent seismic reflection results and their bearing on deep crustal structure, see Barazangi and Brown (1986a,b) and Matthews and Smith (1987). Our approach will be to compile lower-crustal velocity data from over 90 wide-angle seismic studies and compare them to laboratory-measured rock velocities in order to constrain lower-crustal composition. We have divided the seismic profiles according to tectonic environment

in Continental Lower Crust, D.M. Fountain, R. Arculus, and R. Kay, eds., Elsevier, Amsterdam, p. 1–43, 1992.

(e.g., shields, rifts, etc.) in order to seek systematic velocity patterns. The theme that emerges from this compilation is that the lower continental crust is characterized by considerable diversity, but a diversity which can be characterized by current seismic techniques.

Historically, the concept of a distinct seismic lower crust stems from the work of Conrad (1925), who analyzed the traveltimes of earthquake waves and discovered a layer above the Moho with a seismic P-wave velocity (V_p) between that of the upper crust (6.0 km/s) and upper mantle (8.0 km/s). [The Moho itself, the level at which seismic P-wave velocity abruptly increases to about 8.0 km/s, had only recently been discovered by Mohorovičić (1910); for a historical review of Moho studies, see Jarchow and Thompson (1989).] This layer subsequently came to be identified with a basaltic layer (velocity about 6.5 km/s) underlying a supposedly ubiquitous Conrad discontinuity (Jeffreys, 1926). Even today, the term "seismic lower crust" is sometimes carelessly used in this context. The extreme diversity of crustal structure encountered in recent high-resolution seismic experiments, however, underscores the need to abandon such simplifications (e.g., Litak and Brown, 1989). In this review, we have adopted a more flexible definition of the seismic lower crust, as described below.

We begin with a brief overview of the source of wide-angle seismic data, the source of our *in situ* velocity information.

2. Wide-angle seismic data

Traditionally, seismic studies of the deep continental crust have been classified into two categories, refraction and reflection, depending on their acquisition parameters. Refraction data are recorded to long shot-to-receiver offsets (e.g., up to 200–300 km) but generally with sparse receiver spacing (on the order of 1–5 km) and shot spacing (20–100 km). Normal reflection data, in contrast, are typically recorded with denser shot (50–500 m) and receiver spacing (25–100 m), but to much smaller offsets (2–10 km). As a result of these contrasting recording geometries, reflection and refraction data have complementary strengths: reflection data provide a structural image of the crust — that is, shapes of major impedance contrasts — while refraction data provide an estimate of the seismic velocity distribution in the crust. In recent years, as the number of deep crustal reflection and refraction experiments has increased greatly, there has been increasing recognition that, in order to best characterize the deep crust at a given location, both types of data must be collected (e.g., Mooney and Brocher, 1987). Moreover, the traditional differences between refraction and reflection data are becoming blurred with progressive increases in the shot and receiver spacing of refraction experiments and the maximum offsets of reflection experiments. Our interest in this paper is in refraction, or wide-angle, data, as these are the data that yield information on velocities within the lower crust. Below we give a brief summary of the acquisition and interpretation of wide-angle seismic data; for a more detailed review of seismic methods, see Mooney (1989).

2.1. Acquisition

Wide-angle seismic data can be acquired both onshore and offshore; the fundamental requirement is that a sufficient number of receivers exists at offsets large enough to record identifiable, post-critical reflected and refracted phases from the crust and upper mantle. The most common method used during land experiments is to record seismic energy from large chemical explosions (shots) with a large number (>100) of portable instruments, spaced at

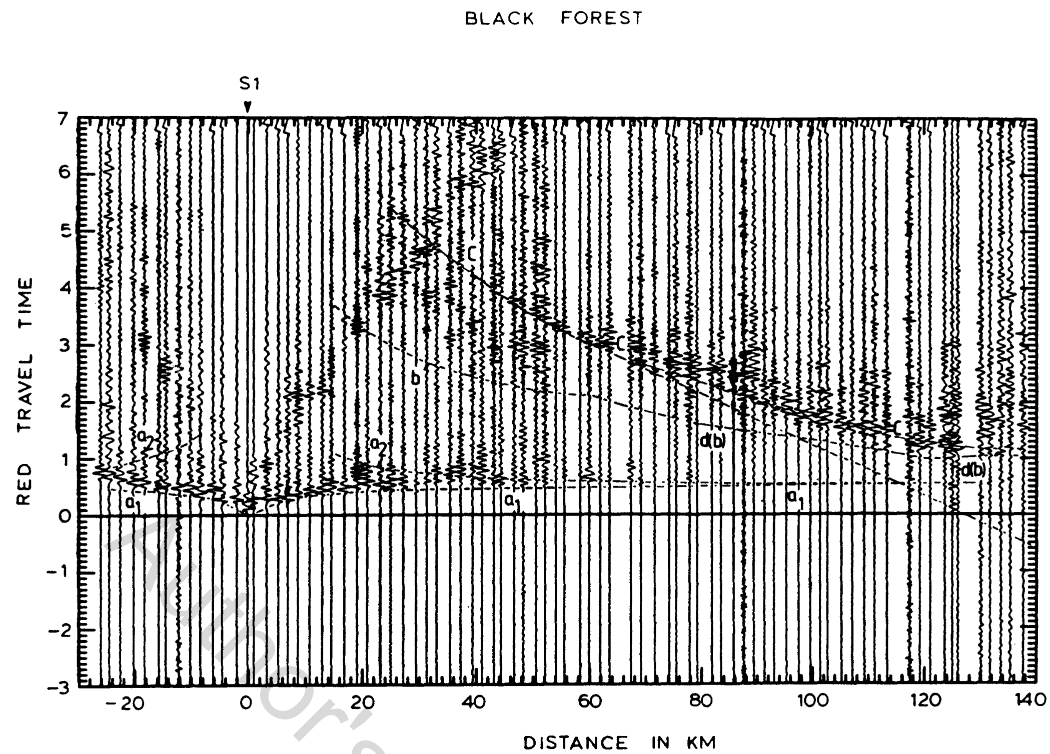

Fig. 1-1. P-wave refraction data from the Black Forest, southwestern Germany, after Gajewski and Prodehl (1987). Vertical-component seismic traces are plotted according to distance from the shotpoint (*S1*). An offset-dependent static shift (Dist/V_r) has been applied to each trace, using a reduction velocity (V_r) of 6.0 km/s; phases with apparent velocity equal to the reduction velocity plot horizontally. Predicted traveltimes of refracted (a_1, $d(b)$) and reflected (a_2, b, c) phases, calculated from the model in Fig. 1-3a, are shown.

regular intervals along a linear profile. The data for a given shot are then plotted as a seismic record section, in which each trace represents energy recorded by a single instrument, plotted as a function of its distance from the shot. A good example of this kind of data, collected in southwestern Germany by Gajewski and Prodehl (1987), is shown in Figure 1-1.

In the marine environment, where it is impractical to deploy large numbers of closely spaced receivers, a relatively new method has been developed to acquire wide-angle seismic data. Large airgun arrays, such as are commonly used in multichannel seismic reflection surveys, are towed behind a ship and detonated at regular intervals (50–100 m). The energy from these airgun pops is recorded on several (5–10) ocean-bottom instruments. In this case, the data from a given instrument are plotted as a seismic record section, in which each trace represents energy from a separate airgun pop, plotted as a function of its distance from the instrument. By the principle of reciprocity, such a receiver gather can be treated in exactly the same manner as a shot gather recorded by many instruments.

Both of the above examples are plots of compressional (P) waves; shear (S) waves, however, can also be recorded in wide-angle experiments. An example of coincident wide-angle compressional- and shear-wave data, recorded in Southwest Germany, is shown in Figure 1-2. Shear waves are transverse waves — that is, the direction of particle motion is perpendicular to the direction of propagation — so that they are best recorded on horizontal-component instruments; however, they are sometimes clearly visible on vertical-component

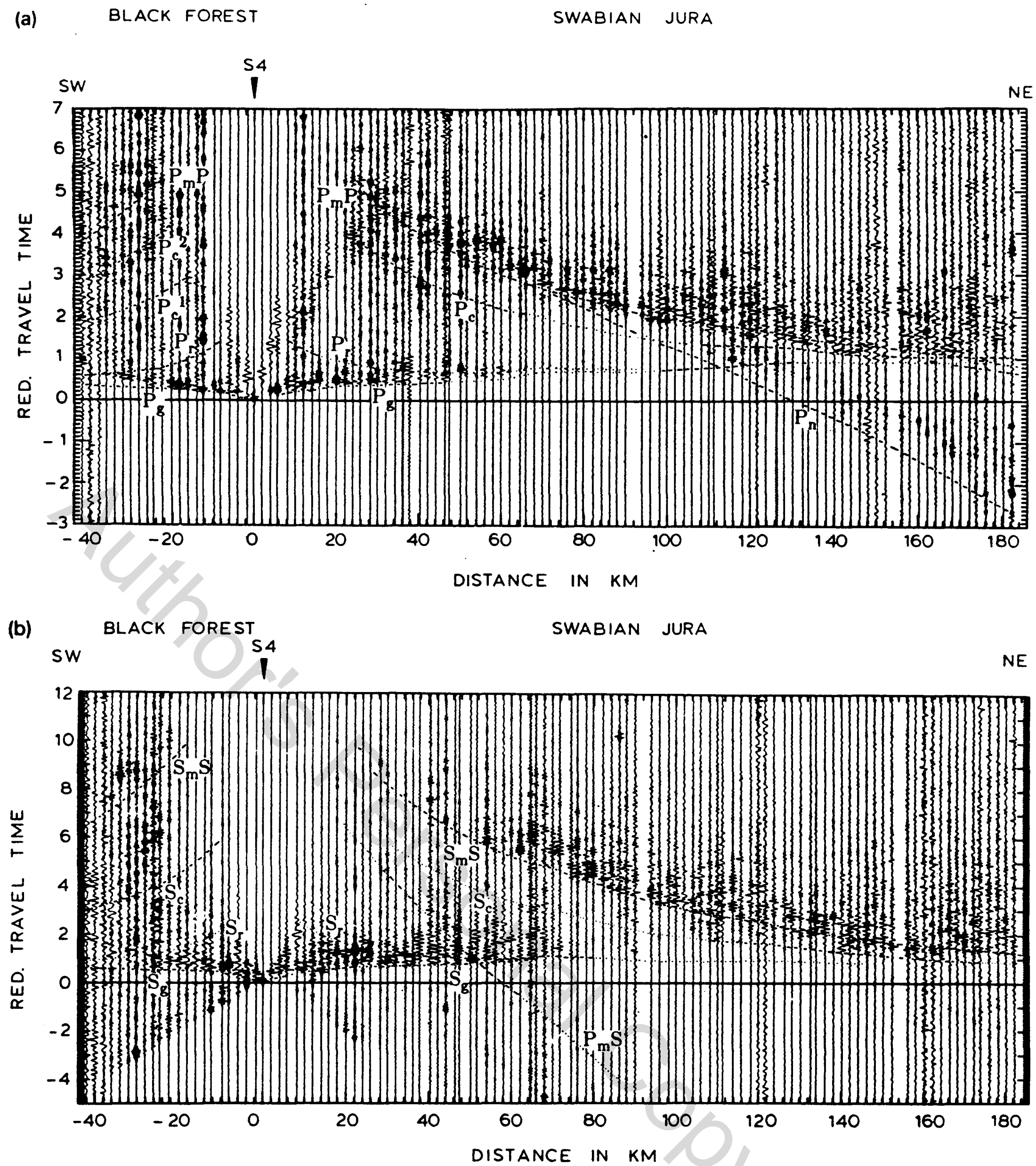

Fig. 1-2. (a) P-wave data (vertical component) from shot U-S4, after Gajewski et al. (1987). Traveltimes of refracted (P_g, P_n) and reflected (P_r, P_c) waves are shown.
(b) S-wave data (horizontal component) from shot U-S4, after Holbrook et al. (1988). Data are plotted with a reduction velocity of 3.46 km/s and a compressed time axis for easier comparison with P-wave record section (Fig. 1-2a).

instruments as well (e.g., Grad and Luosto, 1987). They are easily identifiable on the basis of their slow phase velocities (about $V_p/1.73$). Because shear and compressional waves sense somewhat different physical properties of the rocks through which they propagate, joint P and S interpretations provide more information on crustal composition than P-wave studies alone. Unfortunately, very few interpretations of wide-angle shear waves exist, because of several factors: (1) the difficulty in consistently generating strong shear-wave energy with explosive sources; (2) the paucity of horizontal-component portable seismographs, especially in the U.S.; and (3) the failure of interpreters to routinely look for shear waves in their data.

2.2. Interpretation

Methods for deriving seismic velocity structure from wide-angle seismic data can be divided into one- and two-dimensional techniques. One-dimensional techniques, which assume a laterally uniform velocity structure, include forward traveltime and amplitude modeling (e.g., Fuchs and Müller, 1971), Wiechert-Herglotz inversion (Bullen and Bolt, 1985), and τ_p inversions (e.g., Diebold and Stoffa, 1981). These techniques offer several advantages that two-dimensional methods lack: they are relatively quick and easy to implement, and the latter two provide formal error estimates. One-dimensional methods are limited, however, by their assumption of lateral homogeneity: in regions with significant lateral variability (such as that caused by dipping layers, fault-bounded structures, igneous intrusions, and sedimentary basins) one-dimensional methods yield approximate, or even misleading, results. Therefore, except where there is independent evidence (e.g., geologic, gravimetric, or magnetic) for lateral homogeneity, or where seismic data are unreversed (i.e., only observed in one direction), one-dimensional methods are usually used to provide starting models for two-dimensional modeling.

Two-dimensional interpretation of wide-angle seismic data generally consists of three steps: identification of seismic phases, iterative forward modeling of traveltimes, and calculation of synthetic seismograms. Although these steps proceed roughly in the order they are listed, they are not strictly sequential; rather, they form a continuous feedback loop, where the results of one step often force an earlier step to be repeated. For example, the discovery of an inconsistency in the predicted traveltimes on reversing shots may result in a modified phase correlation; or the comparison of synthetic seismograms to observed amplitudes may necessitate changes in the velocity model which, in turn, require renewed traveltime modeling.

The primary method used for the calculation of traveltimes in a velocity model is the raytracing technique developed by Cerveny et al. (1977). In this method, Snell's Law is used to trace a parcel of energy propagating perpendicular to a wavefront (a ray) through a velocity model consisting of layers or blocks of relatively constant velocity. Traveltimes are calculated by integrating slowness (1/velocity) along the raypath, and amplitudes are determined by applying the Zoeppritz equations (e.g., McCamy et al., 1962) at layer boundaries and calculating the geometrical spreading of adjacent rays (McMechan and Mooney, 1980). Because the raytracing method is based on asymptotic ray theory (i.e., a high-frequency solution to the wave equation), it cannot be used to model such phenomena as diffractions or surface waves. For the applications of crustal seismology, however, these limitations are more than compensated for by the ray method's power in modeling laterally varying structures. Figure 1-3a shows an example of a velocity model derived by raytracing from the Black Forest refraction data of Figure 1-1 (Gajewski and Prodehl, 1987). An idea of the ray coverage provided in this type of experiment can be gained from the ray diagram of Figure 1-3b; the synthetic seismograms calculated from the velocity model (Fig. 1-3c) compare quite favorably with the data (Fig. 1-1).

Workshops on crustal seismology (e.g., Finlayson and Ansorge, 1984; Mooney and Prodehl, 1984) have demonstrated that the greatest uncertainty in forward modeling results from the first, crucial step: phase correlation. Because this is essentially a subjective step, dictated by the experience and judgment of the interpreter, it is difficult to quantify errors in velocity

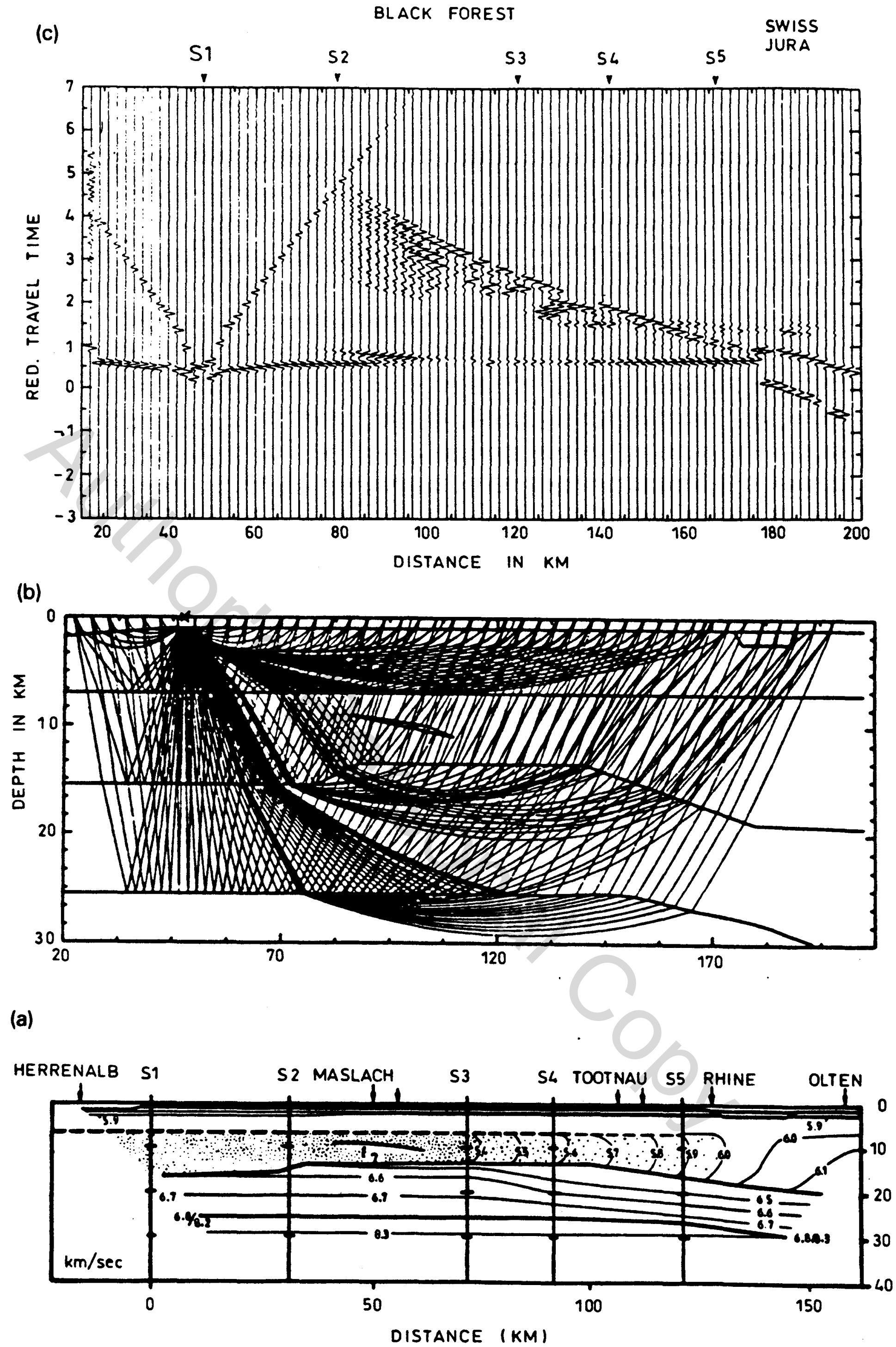

Fig. 1-3. (a) P-wave velocity model for Black Forest (Gajewski and Prodehl, 1987), developed by trial-and-error two-dimensional raytracing. Velocities shown are in km/s.
(b) Raytrace diagram for shot S1 and the P-velocity model of Fig. 1-3a, from Gajewski and Prodehl (1987).
(c) Synthetic seismogram section for Black Forest data (S1), from Gajewski and Prodehl (1987).

models derived by forward modeling. The usual approach is to perturb the velocity model until a significant discrepancy with the observed data is reached; this approach, however, only provides a measure of the error bounds for the velocity model based on a particular phase correlation; still greater differences may result from an alternative phase correlation if the seismic data are sufficiently ambiguous. Future experiments should allow some of these uncertainties to be circumvented: the increased shot and receiver spacing envisioned for these experiments will allow less ambiguous phase correlation and enable increased use of automatic imaging methods, thus reducing the reliance on subjective forward modeling techniques.

2.3. Other methods

Although the type of wide-angle refraction/reflection experiment described above has been the standard means of obtaining velocity information on the deep crust, methods that use different acquisition or interpretive techniques do exist. These include expanding-spread profiles, onshore-offshore profiles, teleseismic receiver functions from earthquakes, and, importantly, common-midpoint reflection profiling. Expanding-spread profiles are commonly collected in two-ship marine experiments where the shooting ship and receiving ship steam away from a common midpoint (Stoffa and Buhl, 1979). Onshore-offshore profiles are landward extensions of marine seismic surveys, in which land seismometers record marine explosions or airgun pops (e.g., Avedik et al., 1984; Gohl et al., 1991). Finally, recordings of teleseismic earthquake waves can be used to supplement wide-angle seismic experiments. In the receiver function method, the teleseismic waveform is modeled to derive a relatively low-resolution one-dimensional crustal structure beneath the recording station (Zandt and Owens, 1986). Because this method is inexpensive and can provide information on the crustal shear-velocity structure, it will probably become a more common complement to wide-angle experiments.

3. Middle- and lower-crustal velocities

The principal goal of this review is to present a summary of continental, middle- and lower-crustal seismic velocities in various tectonic environments, as determined by wide-angle seismic profiling. In choosing velocity models to include in our compilation, we have attempted to strike a balance between selectivity and completeness. Our data base is thus heavily weighted toward studies published in the last decade, when data quality and interpretational techniques improved significantly, though in a few cases we included older or lower-quality data for completeness. In all, our compilation includes results from more than 90 published and unpublished seismic studies (Table 1-1).

In carrying out our compilation, we chose to divide the deep crust into the "middle crust" and the "lower crust", for two reasons. First, in many regions there is no neat division of upper from lower crust. Rather, the deep crust may comprise two distinct velocity layers, or the crust may be best parceled into thirds, with an upper, middle, and lower crust. Second, we expect that many of the processes which create or modify the lower crust will also affect the middle crust, so that a compilation of the velocity structure immediately above the lowermost crust may prove illuminating. We define the middle and lower crust as follows:

(1) In regions where there is no sharp velocity discontinuity (Conrad) near the middle of the crust, the lower 50% of the crust is defined as the lower crust.

TABLE 1-1

References used in P-velocity compilation

Reference	Environment	Quality	Velocity (km/s)
Asano et al., 1985	arc	4	6.8
Azbel et al., 1989	shield	3	6.7–7.0, 7.3
Bamford et al., 1978	Paleozoic	4	7.0
Banda and Ansorge, 1980	Paleozoic	4	6.7
Banda et al., 1981	Paleozoic	4	6.9
Bartelsen et al., 1982	Paleozoic	3	6.2
Barton and Matthews, 1984	rift, passive margin	4	6.5, 6.8
Beaudoin, 1989	rift	1	6.4
Berry, 1973	shield, platform	3	7.2–7.3
Blümling et al., 1985	forearc	3	5.4
Boland and Ellis, 1989	shield	2	7.4–7.5
Braile et al., 1974	rift	3	6.9
Braile et al., 1982	volcanic	3	6.8
Catchings and Mooney, 1988a	volcanic, rift	1	7.5
Catchings and Mooney, 1988b	volcanic, rift	1	7.4
Catchings and Mooney, 1990	rift	2	6.6, 7.4,
Clowes et al., 1987	platform, Paleozoic	3	6.7, 7.4
Colburn and Mooney, 1986	forearc	1	7.2
Cumming et al., 1979	continent collision	3	6.9
Davydova et al., 1985	platform	3	6.6, 6.8, 7.2
Deichmann et al., 1986	continent collision	3	7.1
Egger et al., 1988	rift	3	6.6–6.9, 7.5
EUGENO-S, 1988	shield, platform, rift	1	6.3–6.9
Finlayson et al., 1980	Paleozoic	4	7.4
Finlayson, 1982	shield	4	7.4
Finlayson and Leven, 1987	platform	3	6.8
Finlayson et al., 1984	platform	4	6.8, 7.1
Fuis et al., 1984	rift	2	7.1
Gajewski and Prodehl, 1987	Paleozoic	1	6.6–6.8
Gajewski et al., 1987	Paleozoic	1	6.4–6.7
Gaulier et al., 1988	passive margin	4	6.4, 6.8, 7.2
Ginzburg et al., 1981	rift	3	6.6
Ginzburg et al., 1985	rift	2	6.5
Goldflam et al., 1977	shield	4	6.8
Grad and Luosto, 1987	shield	1	7.3
Guterch et al., 1983	platform, Paleozoic	4	7.0, 7.3–7.4
Hall and Hajnal, 1973	platform	4	7.0
Hennet et al., 1991	Paleozoic	2	6.8
Holbrook and Mooney, 1987	forearc	1	7.0, 7.2
Holbrook, 1990	rift	1,2	6.6, 7.0–7.2
Howie and Miller, 1988	forearc	2	7.1
Ikami et al., 1985	shield	3	6.9
Iwasaki et al., 1990	arc	1	6.6, 6.8
Jacob et al., 1985	Paleozoic	2	6.8
Jentsch, 1979	shield	4	6.4
Kaila et al., 1981	platform	3	7.0–7.5
Kaila, 1986	volcanic	3	6.9
Kaila et al., 1987	shield	3	6.5
Kaila et al., 1989	shield	2	6.8–6.9
Kan et al., 1986	continent collision	3	6.9–7.0

TABLE 1-1 (continued)

Reference	Environment	Quality	Velocity (km/s)
Károly et al., 1986	continent collision, Paleozoic	4	6.8–6.9, 7.2
Keller et al., 1975	rift	4	6.5
Kondorskaya et al., 1981	continent collision, platform	4	6.7, 7.0
LASE Study Group, 1986	passive margin	3	7.2–7.3
Leaver et al., 1984	arc	1	7.0
Lowe and Jacob, 1989	Paleozoic	2	6.9
Luetgert et al., 1987	Paleozoic	1	6.7, 7.0
Luetgert and Mann, 1990	Paleozoic	1	6.8
Luosto and Korhonen, 1986	shield	2	7.2–7.3
Luosto et al., 1989	shield	1	6.9, 7.1
Luosto et al., 1990	shield	1	7.1–7.2
Lutter and Nowack, 1990	Paleozoic	2	6.9
MacGregor-Scott and Walter, 1988	forearc	3	7.2
McCarthy et al., 1989	rift	1	6.6
Mechie et al., 1986	shield	1	6.6–6.8
Mereu et al., 1986	shield	3	6.6, 6.9–7.0
Mooney and Prodehl, 1978	Paleozoic	4	6.7
Mooney et al., 1983	rift	1	7.3
Mooney et al., 1985	shield	1	7.0, 7.3–7.4
Morel–à-l'Huissier et al., 1987	platform	3	7.0–7.2
Mueller et al., 1973	Paleozoic	3	7.1
Mykkeltveit, 1980	Paleozoic	4	7.0
Pakiser and Brune, 1980	arc	4	6.9
Pavlenkova, 1979	platform	4	7.0–7.1, 7.3
Powell and Sinha, 1987	Paleozoic	3	6.7
Prodehl et al., 1984	Paleozoic	4	7.3
Research Group for Seism., 1973	arc	4	6.7–6.8
Sapin et al., 1985	continent collision	4	7.5
Sinno et al., 1986	rift	3	6.7
Sollogub et al., 1973	shield	3	6.8, 7.0
Sparlin et al., 1982	volcanic	3	6.8
Stauber, 1983	rift	3	6.7
Tarkov et al., 1981	shield	4	7.3
Teng et al., 1985	continent collision	3	6.0, 6.7
Trehu and Wheeler, 1987	forearc	3	5.0
Trehu et al., 1989	passive margin	3	7.3–7.4
White et al., 1987	passive margin	3	7.2–7.3
Wilson et al., 1991	rift	1	6.6
Yan and Mechie, 1989	continent collision	2	6.4
Yuan et al., 1986	continent collision	4	6.7, 7.4
Zeis et al., 1990	Paleozoic	2	6.6–6.8
Zelt and Ellis, 1989	platform	1	7.1–7.2
Zucca, 1984	rift	3	6.2

Quality = quality factor (1 = excellent; 2 = good; 3 = fair; 4 = poor).

(2) In regions where there is one velocity layer beneath a Conrad discontinuity, that layer is defined as the lower crust.

(3) If there are two distinct velocity layers beneath a Conrad discontinuity, the middle crust is defined as the layer immediately beneath the Conrad, the lower crust as the layer immediately above the Moho.

TABLE 1-2

Seismic properties of the middle and lower crust

	Shield	Platform	Paleoz	Cont–cont	Volcanic	Rifts	Arcs	Forearcs	Passive
Cross-sectional area surveyed ($\times 10^3$ km^2)									
middle	93	48	47	30	10	34	10	2	0.3
lower	129	46	41	46	16	50	16	3	8
V_p, lower crust (km/s)									
range	6.4–7.5	6.6–7.5	6.2–7.4	6.0–7.5	6.8–7.5	6.2–7.4	6.6–7.0	5.1–7.5	6.4–7.4
mode	6.8, 7.2	6.7, 7.2	6.7	–	6.8, 7.5	6.7, 7.3	6.8, 7.0	7.2	6.5, 7.3
V_p, middle crust (km/s)									
range	6.3–7.0	6.1–7.3	5.4–6.8	6.1–6.6	6.1–6.8	5.5–6.7	6.1–6.6	6.5–6.7	6.8
mode	6.6	6.5	6.4, 6.7	6.2, 6.5	6.5, 6.8	6.2, 6.6	6.1, 6.6	6.6	6.8
V_s, lower crust (km/s)									
range	4.1	4.0	3.6–4.0	–	–	3.3–3.8	–	–	–
mode	4.1	4.0	3.7, 4.0	–	–	3.3	–	–	–
V_s, middle crust (km/s)									
range	4.0	–	3.3–3.7	–	–	3.5	–	–	–
mode	4.0	–	3.7	–	–	3.5	–	–	–
Avg. Poisson ratio									
middle	0.26	–	0.23	–	–	0.29	–	–	–
lower	0.27	0.24	0.26	–	–	0.29	–	–	–
Avg. thickness (km)									
middle	14	15	11	14	11	11	20	5	8
lower	16	11	11	18	20	11	16	6	9
Avg. crustal thickness (km)	45	40	34	55	40	32	38	26	24

Shield = Precambrian shields (e.g., Baltic Shield); Platform = cratonal platforms (e.g., Central U.S. Plains); Paleoz = Paleozoic orogenic areas (e.g., Appalachians, Variscan); Cont–cont = continent–continent collision zones (e.g., Alps, Himalaya); Volcanic = volcanic plateaus (e.g., Columbia plateau, Snake River Plain); Rifts = continental rift zones (e.g., Basin and Range province); Arcs = continental and island arcs (e.g., Japan, Sierra Nevada); Forearcs = forearc regions (e.g., Great Valley, Calif.); Passive = passive continental margins (e.g., U.S. East Coast). Area = cross-sectional area of crust (in units of 1000 km^2) surveyed by P-wave studies. P-wave and S-wave velocities (V_p and V_s) in km/s. Average layer thickness and average crustal thickness in km. Values separated by a comma indicate peaks of bimodal distributions.

(4) Finally, where the velocity structure suggests a natural division of the crust into thirds, the lower crust is defined as deepest third, the middle crust as the middle third.

The flexibility of this set of definitions matches the diversity in the velocity models we examined. For clarity, we will use the term "deep crust" when speaking in a general sense, reserving the terms "middle crust" and "lower crust" for use according to the above definitions. Note that these definitions do not tie the top of the lower crust to a particular seismic velocity, but the base of the lower crust — the Moho — is associated with a seismic velocity (namely, mantle velocities of $\geq$7.6 km/s).

After choosing a velocity model for inclusion in our compilation, we divided its deep crust into blocks of relatively constant velocity, following the lateral and vertical heterogeneity of the model. In layers with strong vertical velocity gradients, it was necessary to approximate the gradient with a constant average velocity. We then categorized the block as belonging to the middle or lower crust and tabulated its P- and S-velocity (V_s), Poisson's ratio (σ), thickness, cross-sectional area (i.e. thickness times horizontal extent), and tectonic environment. In order to provide some measure of the variation in data quality among the seismic studies, we also assigned each velocity determination a subjective quality index, from 1 (highest) to 4 (lowest) (Table 1-1). The quality index was determined by acquisition parameters (e.g., shot and receiver spacing), data quality (e.g., signal-to-noise ratio and presence of identifiable phases), and method of interpretation (e.g., raytracing vs. one-dimensional methods; use of synthetic seismograms). In general, data with a quality factor of 1 had a receiver spacing of 1 km or less, a shot spacing of 30 km or less, good signal-to-noise and identifiable phases at offsets of at least 150–200 km, and were interpreted by two-dimensional raytracing to model both travel times and amplitudes.

We chose to tabulate cross-sectional area of deep crustal units as the best available measure of the amount of crust with a given velocity. Insofar as it is a two-dimensional quantity being used to describe a three-dimensional crust, cross-sectional area is an imperfect parameter; unfortunately, this is an inevitable limitation of two-dimensional seismic surveys. Nevertheless, cross-sectional area is an appropriate measure of the block-like bodies that are common representations of the velocity structure of the deep crust.

The results of the compilation are summarized in Table 1-2. Two important points can be drawn immediately from this table. First, the broad ranges of P-velocity displayed in the deep crust indicate considerable diversity (Table 1-2). The evidence for this diversity has been noted on the basis of both seismic reflection (Smithson, 1978) and refraction (Christensen and Fountain, 1975; Smithson and Brown, 1977; Meissner, 1986) data. P-velocities in the lower crust range from about 6.0 km/s to 7.5 km/s, and in the middle crust from about 5.4 km/s to 7.3 km/s. Second, the tabulated values of cross-sectional area surveyed show that existing deep seismic surveys are biased toward some tectonic environments (e.g., shields, platforms, and rifts) at the expense of others (e.g., arcs, forearcs, and passive margins). Since the distribution of seismic surveys does not necessarily follow the global volumetric abundances of crust in different tectonic provinces, some weighting of the compiled velocity data will be required before conclusions regarding overall (deep) crustal composition can be drawn.

In the following section, we will examine the distribution of deep crustal velocities in more detail and attempt to establish a link to deep crustal composition.

4. Seismic velocities: constraints on composition

The compilations of velocity structure presented above are helpful in providing a crude characterization of the Earth's crust in different tectonic environments, but they are of limited use unless they can be interpreted in terms of lithology. In this section we will discuss the usefulness and limitations of seismic velocities for interpreting the composition of the deep crust.

4.1. Summary of laboratory measurements

The seismic P- and S-wave seismic velocities of the deep crust are primarily determined by five factors: mineralogical composition, confining pressure, temperature, anisotropy, and pore fluid pressure. In order to use seismic velocities to draw inferences about the composition of the deep crust, then, we must first estimate (or assume) the contribution of the other four factors. Lithostatic pressures in the deep crust are easily estimated, but temperatures are less well constrained, and even less is known about the anisotropy and fluid content (and pore pressure) of the deep crust. For the purposes of this paper, we will assume an isotropic, dry crust, with the caveat that this assumption may not hold in all places. There is at present little compelling evidence for the existence of widespread anisotropy or pore pressures high enough to significantly alter seismic velocities in the lower continental crust, although these remain open questions. Hyndman and Klemperer (1989) discuss the implications of the assumption that pore pressures are high enough to reduce seismic velocities in the lower crust.

The effects of pressure and temperature on seismic velocity have been well documented by laboratory measurements (for a compilation of results, see Christensen, 1982; for a review of methods, see Christensen and Wepfer, 1989). As confining pressure increases to about 200 MPa, microcracks close, causing P- and S-velocities to increase rapidly (about 0.5–1.0 km/s/100 MPa); at higher pressures, the increase is slight (about 0.02–0.06 km/s/100 MPa for most rock types; e.g., Birch, 1961; Christensen, 1965, 1966a). As temperature increases, velocities decrease, with typical coefficients of about 2.0–6.0 $\times 10^{-4}$ km/s/°C, depending on rock type (e.g., Kern, 1978; Christensen, 1979). Since pressure and temperature both increase with depth in the Earth, their effects on velocity compete. For a typical continental geotherm of about 15°C/km, a crust of uniform lithology will have a constant velocity at mid- and lower-crustal depths for most rock types, while in high heat-flow provinces (25–35°C/km) the temperature effect dominates, causing negative velocity gradients (Christensen, 1979). Because laboratory measurements of temperature coefficients have been made for most major rock types, the chief source of uncertainty in correcting *in situ* velocities for the effect of temperature is estimating the temperature itself (e.g., Lachenbruch and Sass, 1978). An error of 200°C in the temperature estimate for lower crust, for example, results in an error of about 0.1 km/s in the velocity estimate.

Once the effects of pressure and temperature have been accounted for, and assuming isotropy and the absence of high pore pressure, we can consider seismic velocity to be fundamentally a function of mineralogical composition. Because seismic velocity varies from mineral to mineral, ranging from 6.0 km/s for quartz to 8.4 km/s for garnet (e.g., Christensen and Fountain, 1975), it is a useful yardstick of composition. By comparing the velocities determined in field experiments to those measured in laboratory samples, we hope to estimate the gross composition of the deep crust. In order to facilitate that comparison, we have compiled some laboratory-measured physical properties (P- and S-velocity, density, Poisson's ratio, and P-wave anisotropy) of possible mid- and lower-crustal rock types, spanning compositions from felsic to ultramafic, and metamorphic grades up to granulite and eclogite facies (Table 1-3). In this paper, we will use the term "granulite" strictly to describe metamorphic rocks in granulite facies, whereas we will use the term "amphibolite" in two ways: to describe the rock amphibolite, which consists predominantly of amphiboles, and to describe metamorphic rocks of felsic composition in amphibolite facies (i.e., felsic amphibolite-facies gneiss).

Unfortunately, the correlation between P-wave velocity and composition is sufficiently non-unique that such comparisons are limited to rough estimates of crustal composition. As an extreme example, a P-velocity of 5.8 km/s in the mid-crust could correspond to granite, quartzite, or serpentinite (Table 1-3); in this case, auxiliary geologic or geophysical data, such as shear-wave velocities, drill hole data, potential field data, or detailed knowledge of the geologic history of a given area, would be needed to resolve the ambiguity. In the deep crust, there is a fundamental ambiguity between increasing mafic content and increasing metamorphic grade, both of which can raise seismic velocities: there is significant overlap, for example, between the P-velocities of mafic rocks (gabbro, mafic granulite) and metapelites (Table 1-3).

The non-uniqueness of P-velocity values can be partly overcome, however, by the addition of shear-wave velocity information (e.g., Christensen and Fountain, 1975). The relation between P- and S-velocity for a given rock or mineral can be expressed in terms of Poisson's ratio, which increases with increasing P-velocity or decreasing S-velocity. Poisson's ratio varies from about 0.20 to 0.35 in common rock types and is particularly sensitive to quartz content: while most rock-forming minerals have Poisson's ratios around 0.25–0.30, quartz has a value of 0.08 (Birch, 1961).

By enabling the calculation of Poisson's ratio, coincident compressional- and shear-wave data offer a means of distinguishing between felsic (quartz-rich) and mafic (quartz-poor) rocks that would be indistinguishable on the basis of P-velocity alone. This is demonstrated in Figure 1-4, which shows Poisson's ratio as a function of P-velocity for the rock types in Table 1-3. Although the fields plotted in Figure 1-4 do show some overlap, there is a separation of several rock types whose P-velocities overlap completely. In the middle crust, Poisson's ratio is particularly helpful in distinguishing between quartz-rich rocks such as quartzites and granites from quartz-poor rocks such as serpentinite (Fig. 1-4a). Among lower-crustal rocks, metapelites have discernibly lower Poisson's ratios (0.25–0.29) than mafic (garnet) granulites (0.29–0.33); the ambiguity between increasing mafic content and increasing metamorphic grade is thus largely overcome when shear-wave information is available.

Despite the promise of shear-wave information for resolving some of the ambiguity in linking seismic velocity to lithology, disappointingly few field determinations of shear-wave velocity exist at present: compared to over 90 P-wave studies, we found only eleven published studies of wide-angle shear-waves, geographically restricted to rift zones, shields, and Paleozoic crust (Table 1-4). Because these sparse results are of limited general use in constraining deep-crustal composition, our comparison still suffers from considerable non-uniqueness.

4.2. Results

With that caution in mind, then, we will attempt to draw some petrologic conclusions from our velocity compilation. In order to compare field and laboratory measurements, we have

TABLE 1-3

Laboratory-measured physical properties of possible middle and lower crustal rock types

Rock type	N	ρ	V_p	V_s	σ	P-anis	Ref
Mid-crustal rocks							
1. Serpentinite	16	2.59 ± 0.09	5.50 (5.63) ± 0.55	2.71 (2.79) ± 0.44	0.34 (0.34) ± 0.03	6.9 ± 4.0	6,7,9,20,27
2. Quartzite	9	2.57 ± 0.12	5.52 (5.71) ± 0.57	3.57 (3.60) ± 0.41	0.14 (0.17) ± 0.07	2.9 ± 2.9	2,4,5,19,26,28
3. Granite	27 (26)	2.66 ± 0.05	6.07 (6.22) ± 0.23	3.52 (3.57) ± 0.23	0.24 (0.25) ± 0.04	2.1 ± 1.8	2,4,13,17,21,26,27,28
4. Granodiorite	16	2.69 ± 0.07	6.08 (6.26) ± 0.35	3.43 (3.55) ± 0.21	0.27 (0.26) ± 0.02	2.9 ± 0.9	4,9,13,18,21,26
5. Felsic amph. facies gneiss	18 (15)	2.73 ± 0.07	6.18 (6.27) ± 0.17	3.57 (3.61) ± 0.16	0.25 (0.25) ± 0.03	6.8 ± 3.7	5,13,15,17,21
6. Quartz-mica Schist	8 (6)	2.79 ± 0.07	6.26 (6.37) ± 0.11	3.57 (3.62) ± 0.17	0.26 (0.26) ± 0.04	11.6 ± 7.4	5,13,15,21
7. Metagabbro (greensch.)	14 (9)	2.91 ± 0.09	6.59 (6.76) ± 0.30	3.71 (3.76) ± 0.11	0.27 (0.28) ± 0.01	–	9,16
8. Gabbro	33 (15)	2.94 ± 0.09	6.95 (7.12) ± 0.22	3.74 (3.80) ± 0.18	0.29 (0.30) ± 0.02	2.5 ± 1.5	2,4,9,12,13,16,18,19,22,25
9. Amphibolite	11 (10)	3.05 ± 0.10	7.03 (7.05) ± 0.24	3.77 (3.92) ± 0.21	0.30 (0.28) ± 0.02	5.4 ± 5.3	5,12,13,17,18,19,27
Lower crustal rocks							
1. Quartzite (granulite)	17	2.66 ± 0.12	5.82 (5.97) ± 0.22	3.71 (3.75) ± 0.09	0.15 (0.17) ± 0.05	4.0 ± 0.0	2,4,5,19,26,28
2. Felsic amphib. gneiss	16 (13)	2.73 ± 0.07	6.20 (6.36) ± 0.19	3.54 (3.62) ± 0.16	0.26 (0.26) ± 0.03	7.3 ± 3.2	5,13,15,17,21
3. Felsic granulite	13	2.70 ± 0.06	6.25 (6.44) ± 0.11	3.53 (3.64) ± 0.09	0.27 (0.27) ± 0.02	2.8 ± 2.2	3,10,13,21,24
4. Quartz-mica Schist	8 (6)	2.79 ± 0.07	6.29 (6.47) ± 0.12	3.58 (3.66) ± 0.16	0.26 (0.26) ± 0.04	10.7 ± 6.4	5,13,15,21
5. Intermediate granulite	21	2.79 ± 0.11	6.39 (6.59) ± 0.20	3.58 (3.69) ± 0.14	0.27 (0.27) ± 0.03	2.7 ± 1.5	10,13,21,23,24
6. Anorthosite	15	2.80 ± 0.10	6.81 (7.03) ± 0.31	3.65 (3.72) ± 0.20	0.30 (0.31) ± 0.02	2.9 ± 1.6	2,4,13,15,24,27,29
7. Mafic granulite	38	3.03 ± 0.17	6.86 (7.13) ± 0.27	3.60 (3.90) ± 0.22	0.31 (0.29) ± 0.02	2.6 ± 1.7	10,12,13,14,15,20,23,24
8. Amphibolite	13 (12)	3.05 ± 0.09	7.00 (7.14) ± 0.24	3.81 (4.03) ± 0.22	0.29 (0.27) ± 0.02	5.4 ± 5.2	5,13,15,17,18,19,27
9. Metapelite (granulite)	12 (11)	3.10 ± 0.11	7.17 (7.33) ± 0.36	4.03 (4.11) ± 0.21	0.27 (0.27) ± 0.01	5.5 ± 5.5	14,15,20,21,23
10. Pyroxenite	14	3.27 ± 0.04	7.71 (8.00) ± 0.15	4.23 (4.41) ± 0.27	0.28 (0.28) ± 0.04	2.2 ± 1.7	1,2,4,9,12,15,22,26,27
11. Eclogite	24	3.43 ± 0.09	7.94 (8.11) ± 0.28	4.38 (4.54) ± 0.16	0.28 (0.27) ± 0.02	2.4 ± 0.9	18,23,24,27
12. Dunite/Peridotite	18	3.28 ± 0.04	8.02 (8.28) ± 0.23	4.37 (4.61) ± 0.18	0.29 (0.28) ± 0.02	11.6 ± 4.0	1,2,4,6,18,19,22,26,27

Values shown are averages of highest-pressure measurement from each sample within the ranges 3–5 kbar for the middle crust and 4–10 kbar for the lower crust; ranges shown are one standard deviation. Velocities have been corrected for the effect of temperature assuming a stable cratonic geotherm (15°C/km). N = number of samples (number of samples for which S-velocity was measured in parentheses, if different); ρ = density (gm/cm3); V_p = P-wave velocity (km/s); V_s = S-wave velocity (km/s); σ = Poisson's ratio; P-anis = percent P-wave velocity anisotropy. Ref = references: 1, Babuska, 1972; 2, Birch, 1960, 1961; 3, Bonatti and Seyler, 1987; 4, Bonner and Schock, 1981; 5, Christensen, 1966a; 6, Christensen, 1966b; 7, Christensen, 1972; 8, Christensen, 1977; 9, Christensen, 1978; 10, Christensen and Fountain, 1975; 11, Christensen et al., 1975; 12, Chroston and Evans, 1983; 13, Chroston and Brooks, 1989; 14, Evans, 1980; 15, Fountain, 1976; 16, Fox et al., 1973; 17, Hall and Simmons, 1979; 18, Kanamori and Mizutani, 1965; 19, Kern, 1982; 20, Kern and Schenk, 1985; 21, Kern and Schenk, 1988; 22, Kroenke et al., 1976; 23, Jackson and Arculus, 1984; 24, Manghnani et al., 1974; 25, Nur and Simmons, 1969; 26, Schock et al., 1974; 27, Simmons, 1964; 28, Simmons and Brace, 1965; 29, Wang et al., 1973.

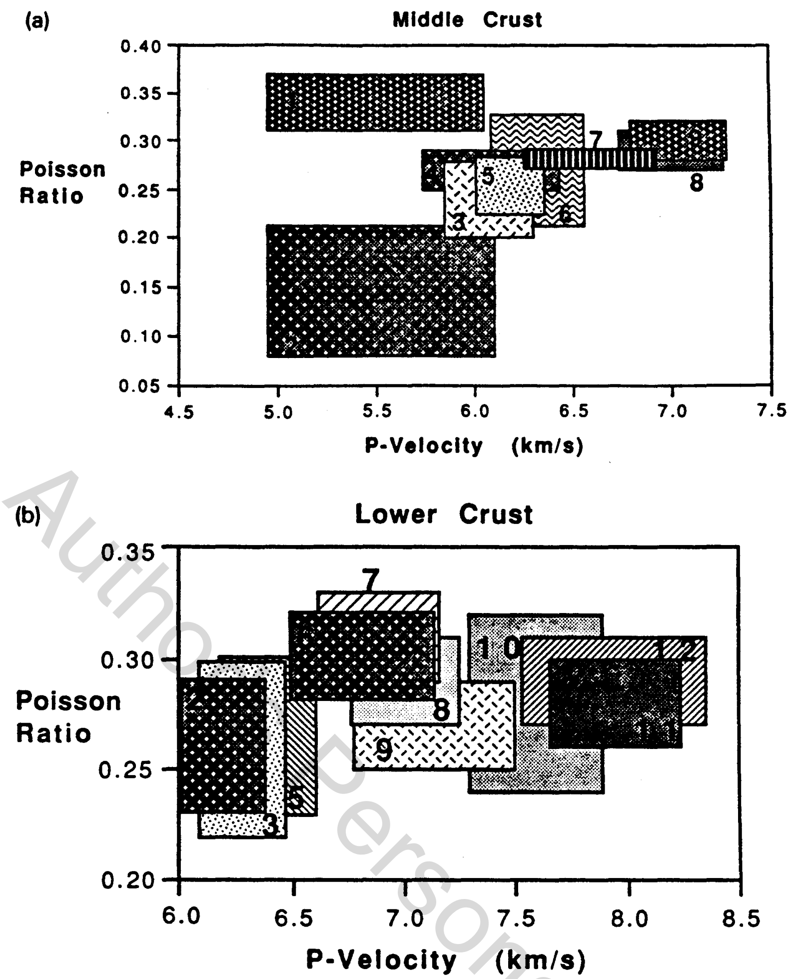

Fig. 1-4. Plots of P-velocity vs. Poisson's ratio for (a) mid-crustal and (b) lower-crustal rock types, from the data of Table 1-3. Width of fields equals two standard deviations; numbers keyed to rock types of Table 1-3. For plot clarity, rock types 1 and 4 (quartzite and schist) are not included in Fig. 1-4b.

TABLE 1-4

References used in S-velocity compilation

Reference	Environment	Quality	S-velocity	σ
Assumpçao and Bamford, 1978	Paleozoic	4	4.0	0.25
Banda et al., 1981	Paleozoic	4	3.9	0.26
Boland and Ellis, 1991	Shield	2	4.2	0.27
Braile et al., 1974	Rift.	4	3.8	0.28
Grad and Luosto, 1987	Shield	1	4.1	0.27
Hall and Hajnal, 1973	Shield	4	4.0	0.24
Holbrook et al., 1988	Paleozoic	1	3.6–3.8	0.24–0.29
Keller et al., 1975	Rift	4	3.5	0.29
Luetgert et al., 1987	Paleozoic	1	3.9–4.0	0.25
Luosto et al., 1990	Shield	1	4.0–4.1	0.26–0.27
Tarkov et al., 1981	Shield	4	4.1	0.26

Quality = quality factor; σ = Poisson's ratio.

plotted the laboratory-determined ranges of the velocities and Poisson's ratios for middle- and lower-crustal rocks (Table 1-3) above histograms of the field-measured values in Figures 1-5 to 1-9. All of the lab-measured velocities shown in these plots, as well as in Table 1-3, have been corrected for temperature using published temperature derivatives (e.g., Kern, 1978; Christensen, 1979) and assuming the stable craton geotherm of Lachenbruch and Sass (1978), which predicts a temperature of about 600°C at a depth of 40 km. This correction, which amounts to about 0.2–0.3 km/s for most rock types in the lower crust, is an average estimate, as temperatures vary with tectonic environment; however, this will not affect our conclusions, since the uncertainty in the temperature correction is less than the observed ranges in lab-measured velocity for any given rock type (Table 1-2).

The summary histograms in Figures 1-5 to 1-7 show a deep continental crust with widely varying seismic properties. In the lower crust, 94% of the P-velocity determinations fall between 6.4 km/s and 7.4 km/s (57% between 6.6 km/s and 7.0 km/s), and there is a clear peak at 6.7–6.8 km/s. In the middle crust, 90% of the P-velocities fall between 6.0 km/s and 6.8 km/s, with a strong peak at 6.5–6.6 km/s. Shear-wave velocities in the lower crust show a range of 3.5 km/s to 4.2 km/s, with most values between 3.9 km/s and 4.2 km/s (Fig. 1-7b); in the middle crust, S-velocities range from 3.3 km/s to 4.0 km/s, with most between 3.7 km/s and 4.0 km/s (Fig. 1-7d). The distribution of Poisson's ratio in the lower crust shows a range of 0.24 to 0.29, with most values from 0.24 to 0.27 (Fig. 1-7c); in the middle crust, most values lie between 0.24 and 0.27, with some low (0.15) and high (0.29) determinations (Fig. 1-7a).

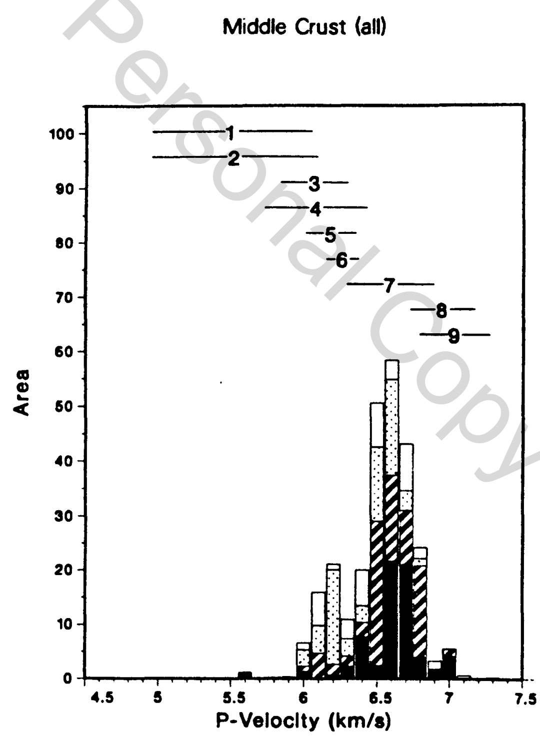

Fig. 1-5. Histogram of cross-sectional area of crust (in km^2 x 10^3) vs. P-wave velocity for the middle crust in all tectonic provinces. Shading indicates quality factor, from highest (1) to lowest (4): 1 = black; 2 = hatchured; 3 = stippled; or 4 = blank. Bars at top show velocity ranges (plus/minus one standard deviation) for possible mid-crustal rock types (Table 1-3): *1* = serpentinite; *2* = quartzite; *3* = granite; *4* = granodiorite; *5* = felsic amphibolite facies gneiss; *6* = schist; *7* = metagabbro; *8* = gabbro; *9* = amphibolite.

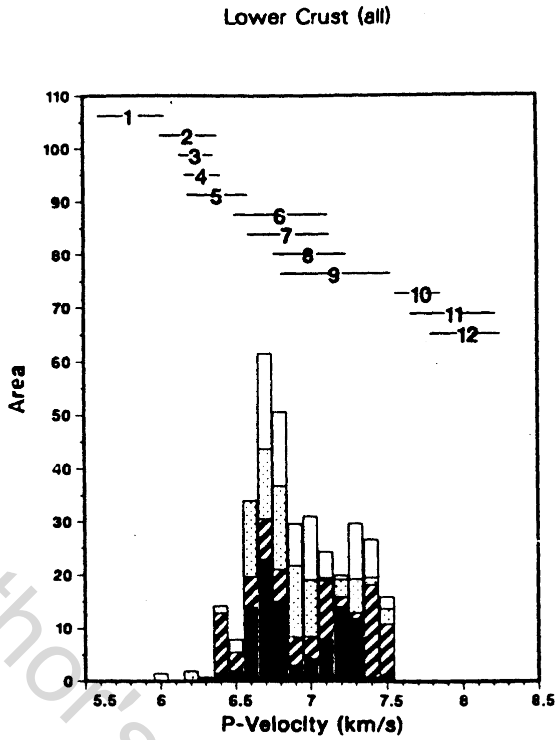

Fig. 1-6. Histogram of cross-sectional area of crust (in $km^2 \times 10^3$) vs. P-wave velocity for the lower crust in all tectonic environments. Shading indicates quality factor (see Fig. 1-5). Bars at top show velocity ranges (plus/minus one standard deviation) for possible lower crustal and upper mantle rock types (Table 2): *1* = quartzite (granulite); *2* = felsic amphibolite facies gneiss; *3* = felsic granulite; *4* = schist; *5* = intermediate granulite; *6* = anorthosite; *7* = mafic granulite; *8* = amphibolite; *9* = felsic and intermediate garnet granulite; *10* = pyroxenite; *11* = eclogite; and *12* = dunite/peridotite.

The large range of P-velocities plotted in Figures 1-5 and 1-6 implies that the deep continental crust must be composed of a diversity of rock types. The span of the lower-crustal velocities, from 6.4 km/s to 7.5 km/s, overlaps the velocity ranges of quartz-mica schist, intermediate and mafic granulites, anorthosite, amphibolite, and metapelites (Fig. 1-6). The lower-crustal velocity distribution has several peaks: there are strong peaks at 6.7–6.8 km/s and 7.2–7.5 km/s, and a subsidiary peak at 7.0 km/s. The low-velocity (6.7–6.8 km/s) peak roughly corresponds to the velocity ranges of anorthosite or mafic granulite, while the high-velocity peak (7.2–7.5 km/s) corresponds to granulite-facies metapelite or pyroxenite. In the middle crust, where the velocity distribution is narrower, the peak at 6.5–6.8 km/s best matches the velocities of greenschist-facies metagabbro, although they also fall within the ranges of quartz-mica schist, gabbro, and amphibolite (Fig. 1-6).

Using the histograms of Figure 1-8 we can draw more detailed conclusions about the average composition of the deep crust as a function of tectonic environment. In each environment, the range of observed velocities in both the middle crust and lower crust requires considerable lateral changes in bulk composition. The strongest manifestation of this is the bimodal distribution of P-velocities in the lower crust of some tectonic environments — shields, platforms, passive margins, and, to a lesser extent, rifts and volcanic plateaus — which indicates strong lateral changes in composition. The high velocities

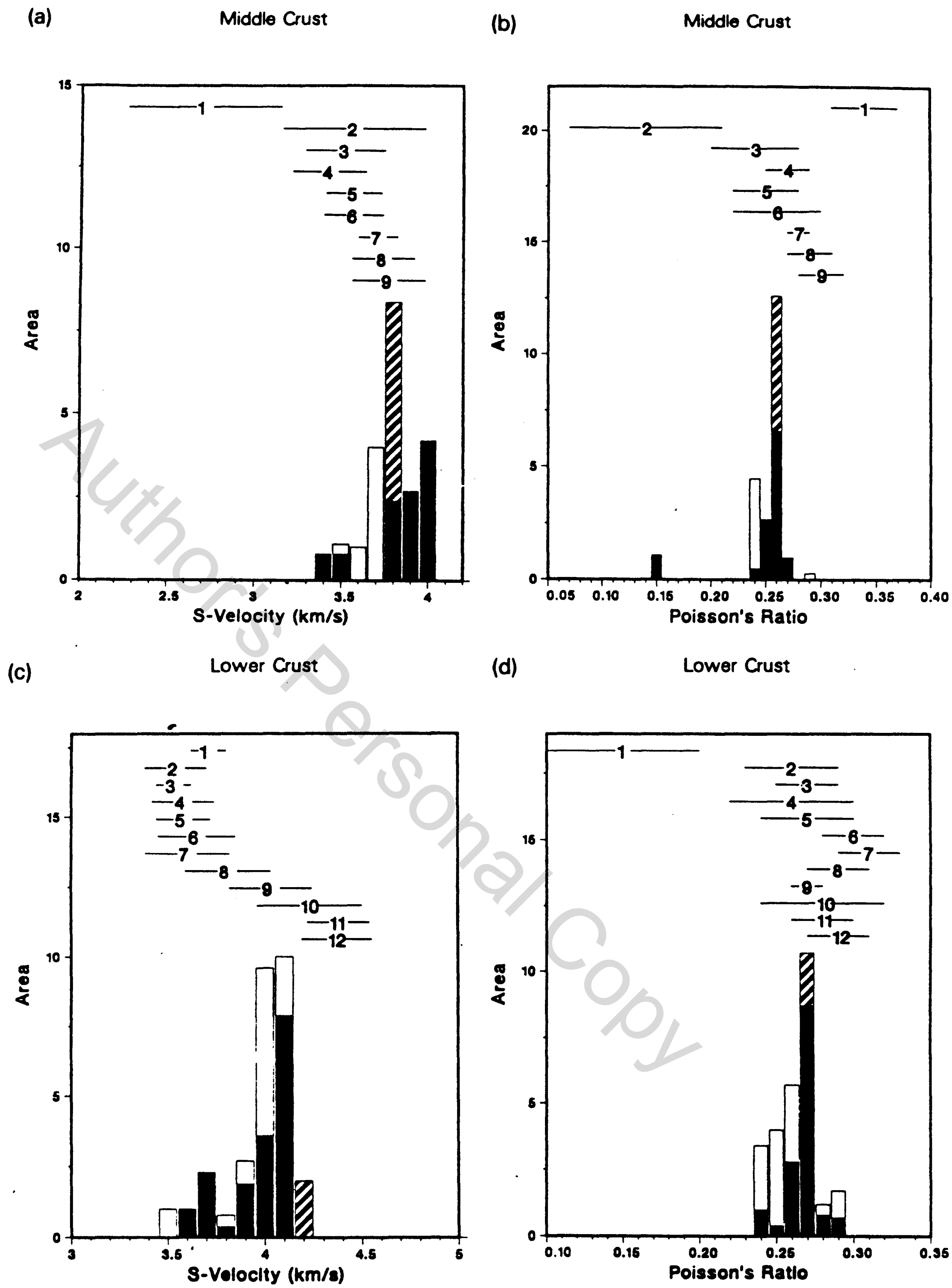

Fig. 1-7. Histograms of cross-sectional area of crust vs. S-wave velocity and Poisson's ratio in the deep crust. (a) S-velocity in the middle crust, (b) Poisson's ratio in the middle crust, (c) S-velocity in the lower crust, (d) Poisson's ratio in the lower crust.

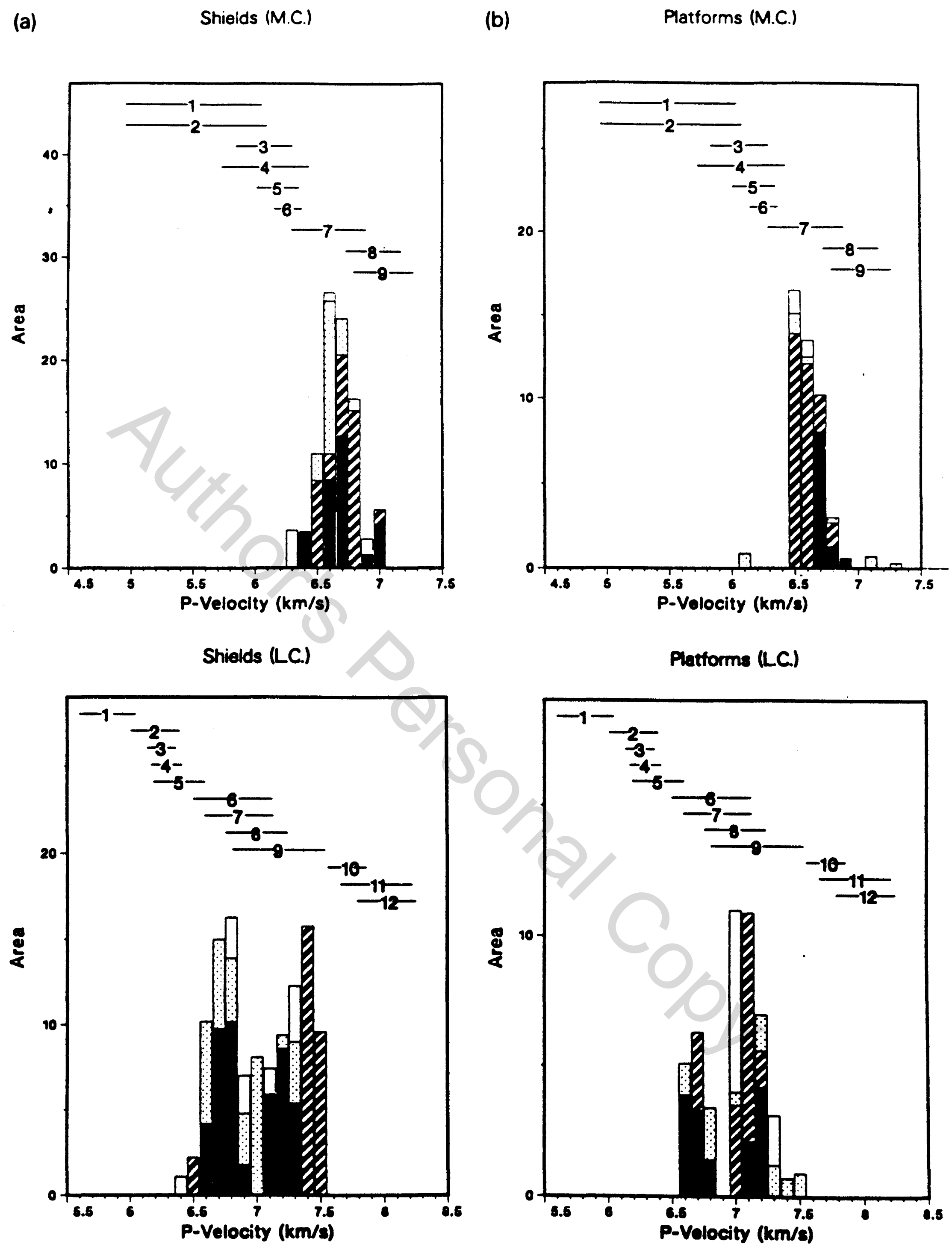

Fig. 1-8. Histograms of cross-sectional area of crust (in km^2 x 10^3) vs. P-wave velocity for the middle crust (M.C.) and lower crust (L.C.), plotted as in Fig. 1-5, for (a) shields, (b) platforms.

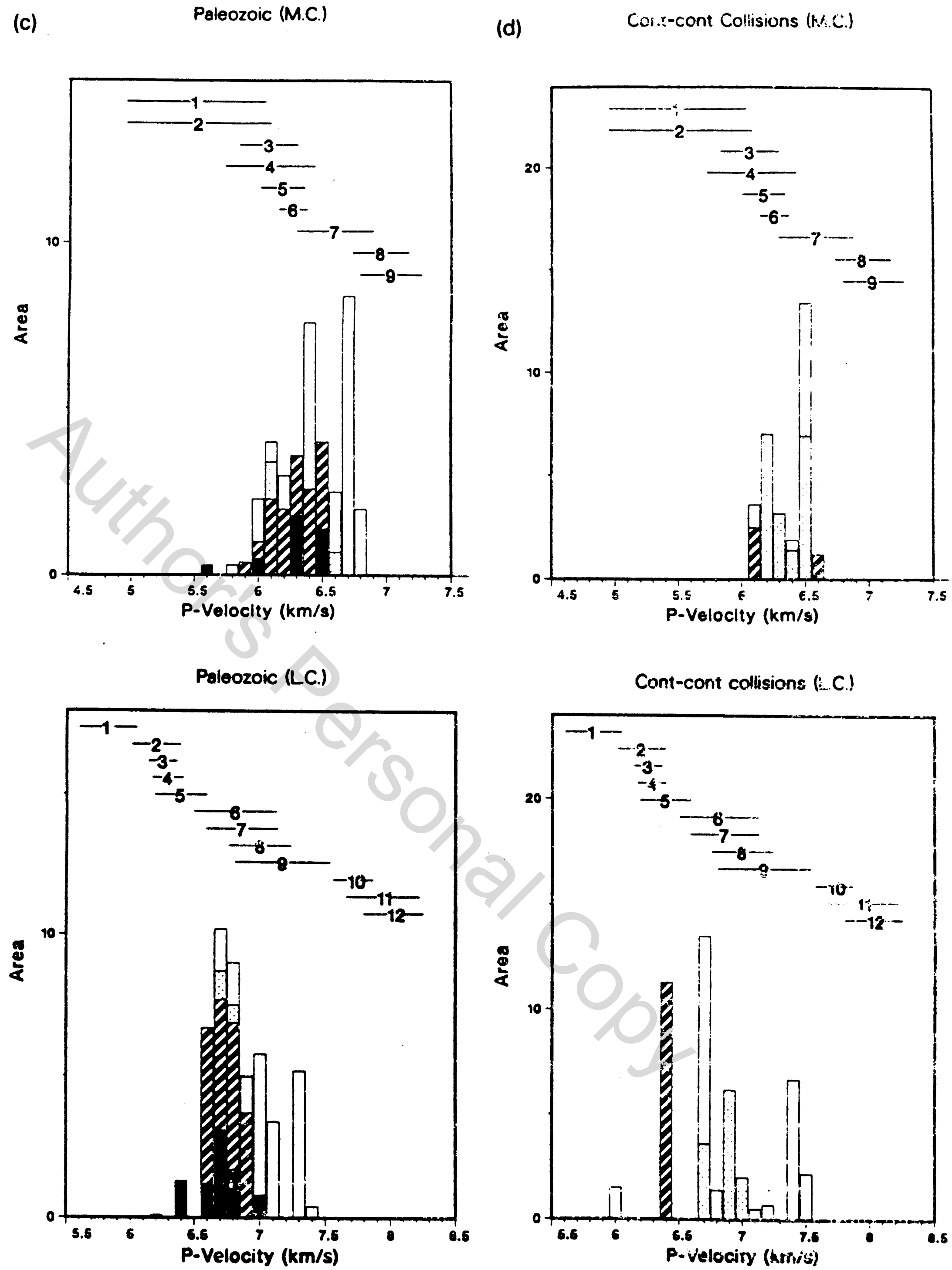

Fig. 1-8 (continued). Histograms of cross-sectional area of crust (in km^2 x 10^3) vs. P-wave velocity for the middle crust (M.C.) and lower crust (L.C.), plotted as in Fig. 1-5, for (c) Paleozoic crust, (d) continent–continent collision zones.

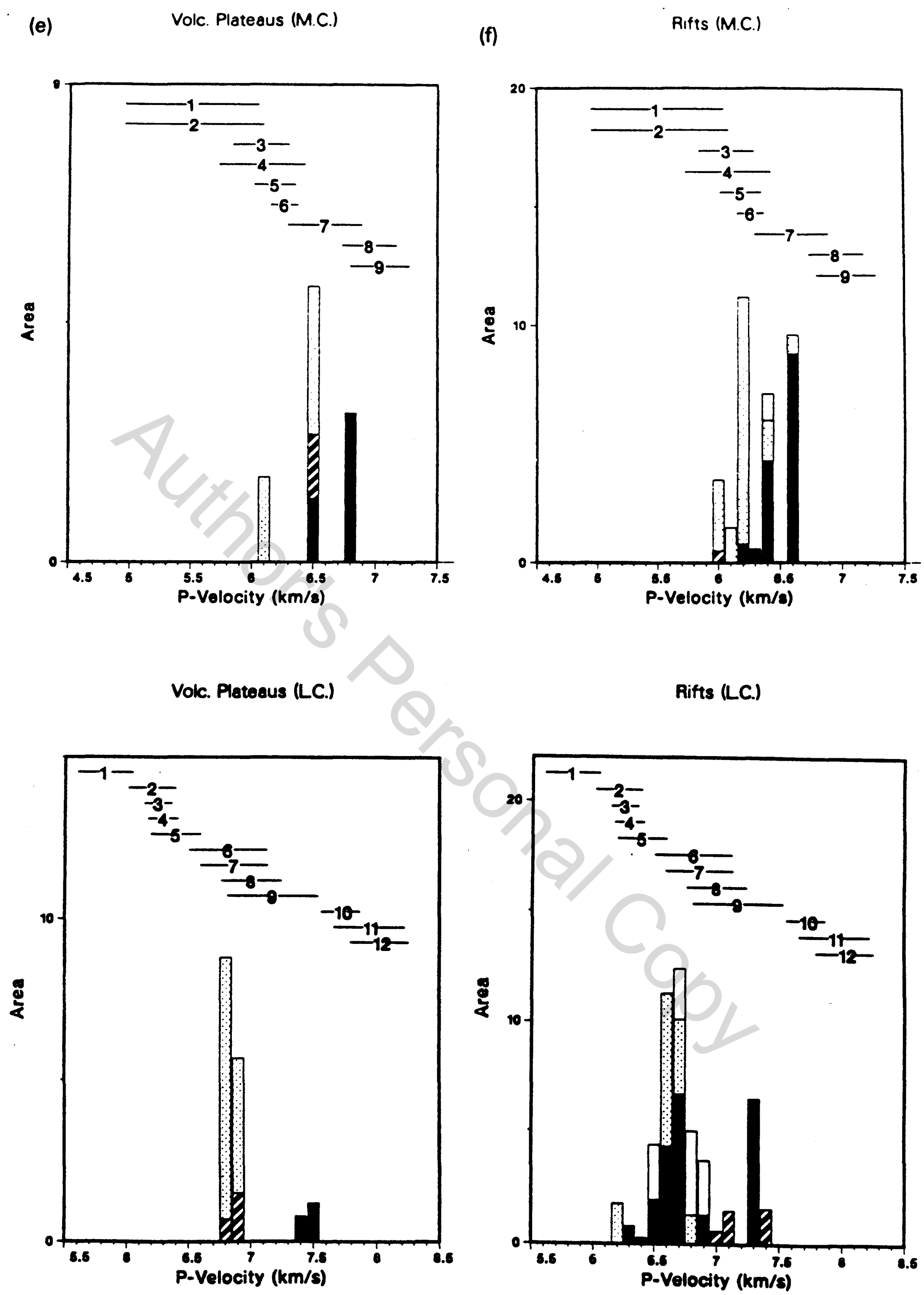

Fig. 1-8 (continued). Histograms of cross-sectional area of crust (in km^2 x 10^3) vs. P-wave velocity for the middle crust (M.C.) and lower crust (L.C.), plotted as in Fig. 1-5, for (e) volcanic plateaus, (f) rifts.

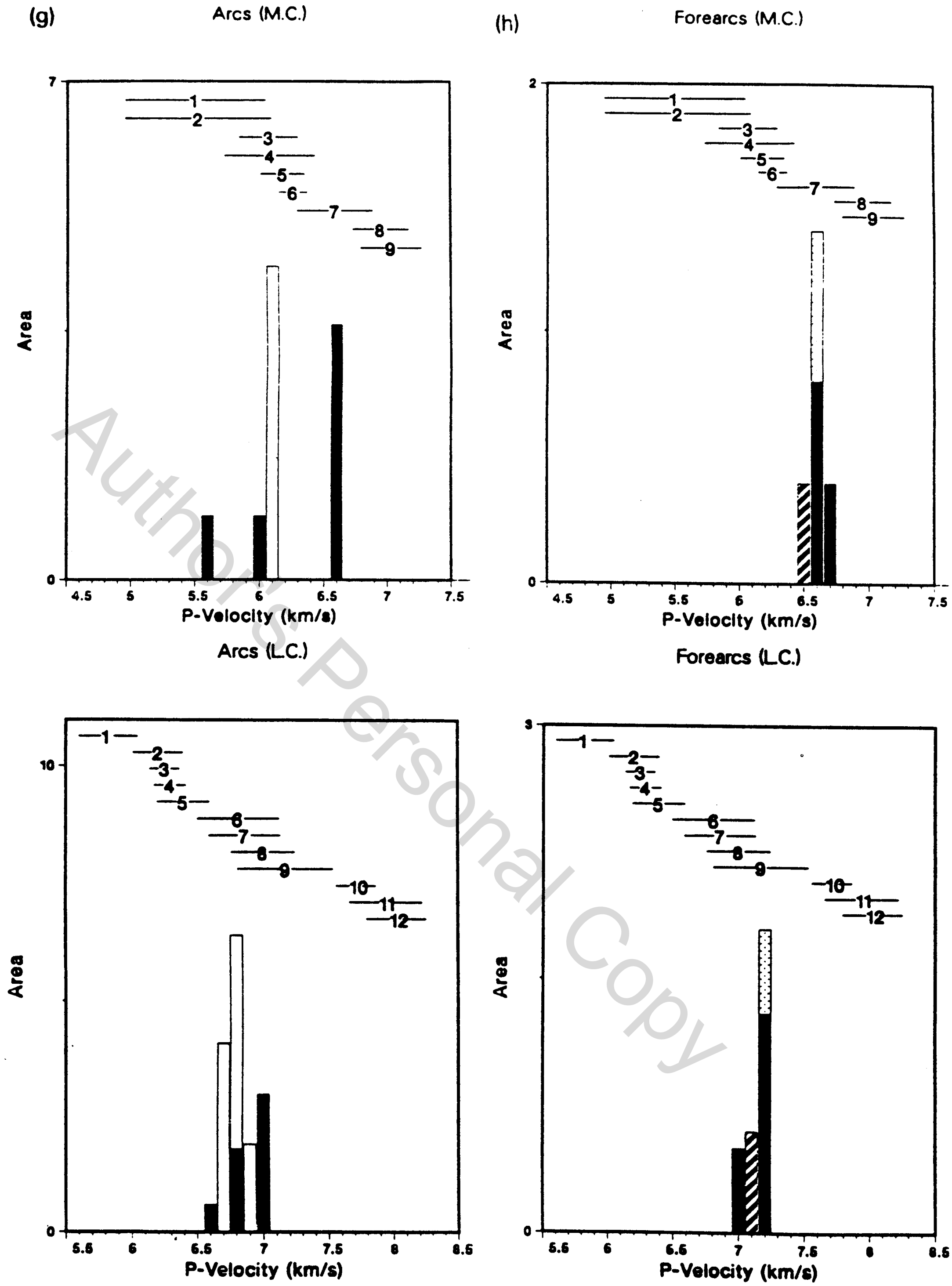

Fig. 1-8 (continued). Histograms of cross-sectional area of crust (in km^2 x 10^3) vs. P-wave velocity for the middle crust (M.C.) and lower crust (L.C.), plotted as in Fig. 1-5, for (g) arcs, (h) forearcs.

(i) Passive margins (L.C.)

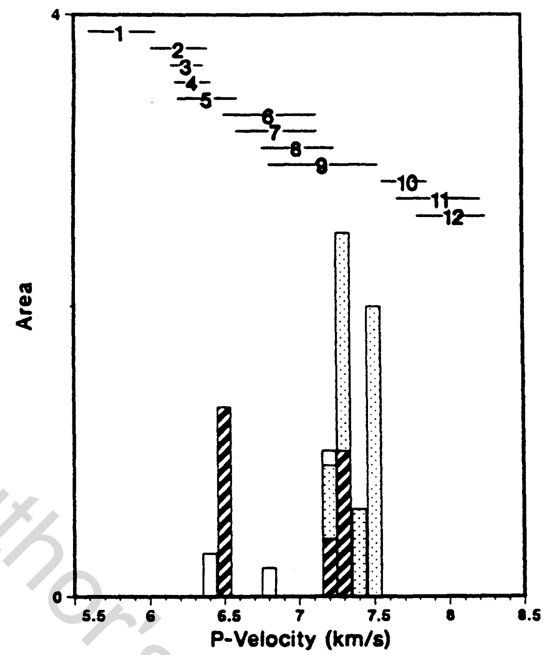

Fig. 1-8 (continued). Histograms of cross-sectional area of crust (in km^2 x 10^3) vs. P-wave velocity for the middle crust (M.C.) and lower crust (L.C.), plotted as in Fig. 1-5, for (i) passive margins.

(7.2–7.5 km/s) in these areas require the presence of metapelite, pyroxenite, or a mixture of mafic and ultramafic rocks. The lower-velocity peaks (6.6–6.8 km/s) are best modeled as mafic granulites, anorthosites, or possibly intermediate granulites. In the middle crust, likely compositions vary from metagabbro (greenschist) in shields, platforms, and some volcanic plateaus, rifts, and continent–continent collision zones, to more felsic compositions (granite, granodiorite, felsic amphibolite-facies gneiss, and schist), in Paleozoic crust and some volcanic plateaus, rifts, and continent–continent collision zones.

These results are summarized in Table 1-5, which shows the rock types best matched by the major peaks in the velocity histograms of Figure 1-8. It is important to keep in mind that this summary represents an average or typical result for each environment — due to the extreme diversity of field-measured velocities, however, these average lithologies may not apply at a particular location. Moreover, a lower crust which can be modeled as having, say, a bulk mafic composition may also contain roughly balanced amounts of felsic and ultramafic rocks. Nevertheless, the comparison of average seismic velocity to laboratory-measured rock velocities provides a useful constraint on the allowable proportions of various rock types in the lower crust.

The broad range of rock types which are possible constituents of the lower crust reflects the non-uniqueness of petrological inferences drawn from P-velocities. Some help can be obtained from the sparse shear-wave (i.e., Poisson's ratio) information available in rifts, Paleozoic regions, and shields (Fig. 1-9). In shields and platforms, the relatively low Poisson's ratios (0.24–0.27) favor less mafic compositions-quartz-mica schists, intermediate granulites, and granulite-facies metapelites. In rifts, the somewhat higher Poisson's ratios favor anorthosites,

TABLE 1-5

Possible bulk composition of middle and lower crust

Middle crust

Environment	serp	qtz	gran	gdior	f.gns	sch	metag	gabb	amph
Shields						□ +	●	□	□
Platforms						□	●		
Paleozoic			□ +	□ +	● +	● +	□	□	
Cont. col.(low)			●	●	●	□			
(high)						□	●		
Volc.(l)			●	●					
(h)						□	●	□	
Rift (l)	□	□ +	●	●	●	□	●	●	●
(h)						● +	● +		
Arcs		□	□	□	□	●			
Forearc					□	●	□		

Lower crust

Environment	qtz	f.gns	fels	sch	int	anor	maf	amp	metap	px	maf+ult
Shields (low)					□	●	●	□	□		
(high)								□	● +	□	●
Platforms (l)					□	●	●	□			
(h)						□	□	●	●		□
Paleozoic					□	●	●	□	□ +		
Cont. col. (l)		□	●	●	●	●	●	●	●		
(h)									□	□	●
Volc. (l)						●	●	●	□		
(h)									□		●
Rift (l)					□	● +	●	□ +			
(h)									●		●
Arcs						●	●	●	●		
Forearc (l)	□										
(h)						●	●	●	●		
Passive (l)					●	□					
(h)								□	●		●

Symbols mark compositions which show good (●) or fair (□) agreement with observed histogram peaks; + denotes compositions favored by available Poisson's ratio data. Low (l) and high (h) refer to separate low- and high-velocity peaks, where appropriate. Compositions in middle crust: serp = serpentinite; qtz = quartzite; gran = granite; gdior = granodiorite; f.gns = felsic amphibolite gneiss; sch = schist; metag = metagabbro; gabb = gabbro; amph = amphibolite. Compositions in lower crust: qtz = quartzite; f.gns. = felsic amphibolite gneiss; fels = felsic granulite; sch = schist; int = intermediate (granodioritic) granulite; anor = anorthosite; maf = mafic granulite; amp = amphibolite; metap = metapelite; px = pyroxenite; maf+ult = mix of mafic and ultramafic rocks.

amphibolites, and intermediate granulites, while in Paleozoic regions, the broad range of Poisson's ratios suggests compositional diversity.

These interpretations are best shown by plotting the field-determined P-velocities and Poisson's ratios from a particular location on the fields of laboratory-measured values, as shown in Figure 1-10 for the Paleozoic crust of southwest Germany (Holbrook et al., 1988), the Ukrainian and Baltic shields (Tarkov et al., 1981; Grad and Luosto, 1987) and the

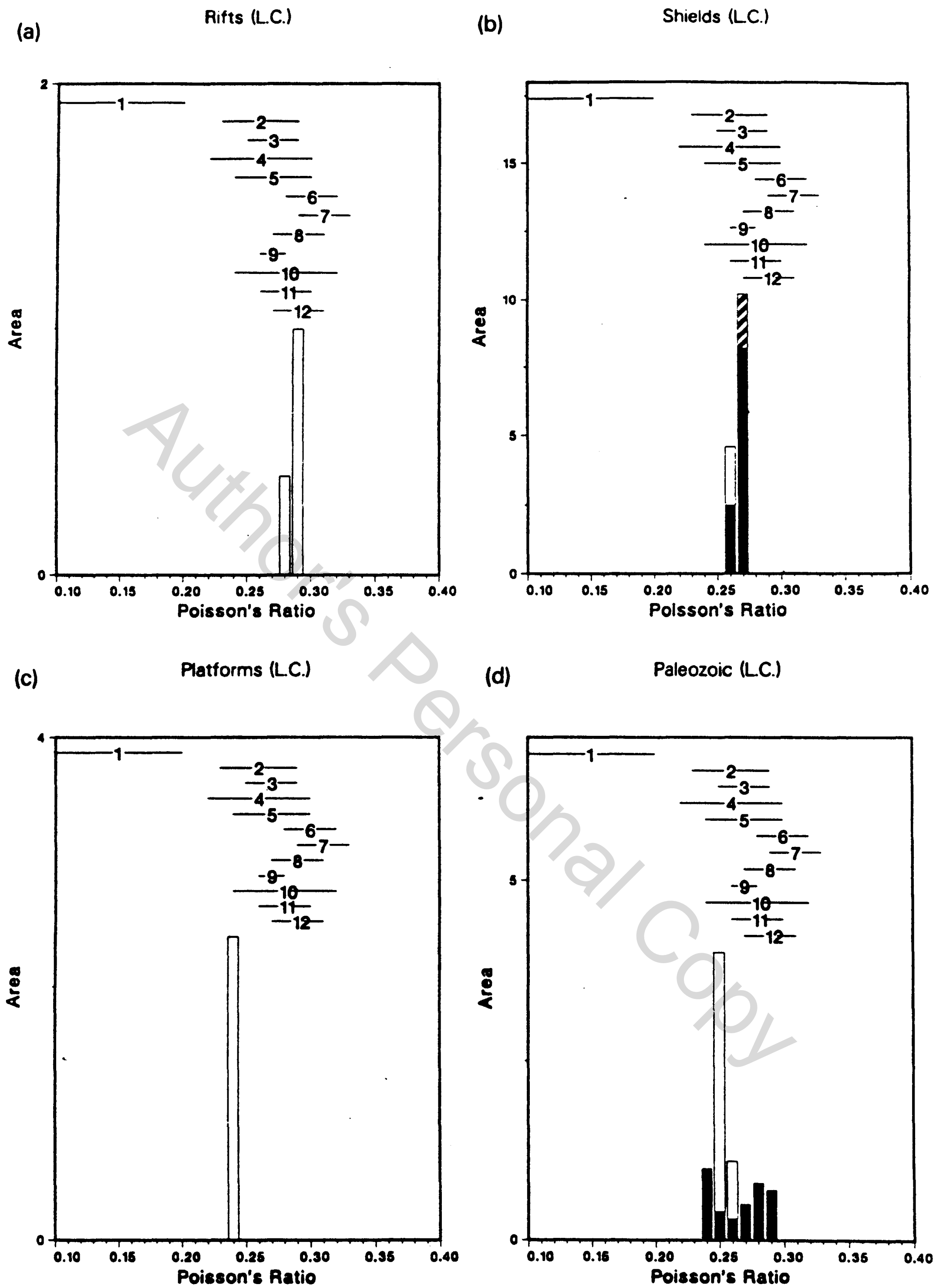

Fig. 1-9. Histograms of cross-sectional area of lower crust vs. Poisson's ratio in (a) rifts, (b) shields, (c) platforms, and (d) Paleozoic crust.

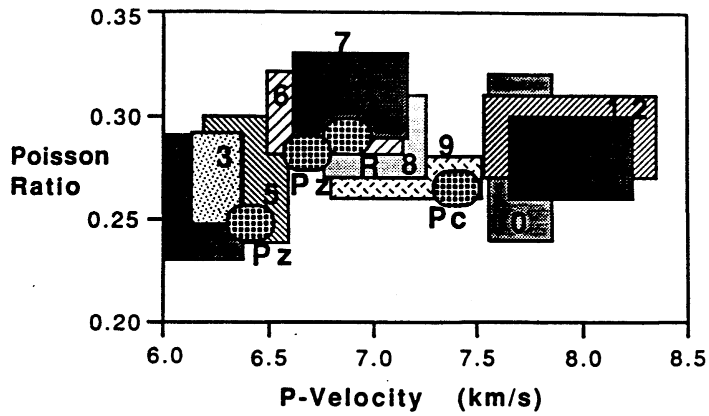

Fig. 1-10. Comparison of field- and laboratory-measured P-velocities and Poisson's ratios. Field-measured data from several areas (cross-hatchured ovals) are plotted on fields of lab-measured data from Fig. 1-4. *R* = rift zone (Basin and Range, Braile et al., 1974); *Pc* = Precambrian shield (Kapuskasing uplift, Boland and Ellis, 1991); *Pz* = Paleozoic crust (Black Forest and Urach areas, Holbrook et al., 1988).

Basin and Range rift zone (Braile et al., 1974). In the lower crust of Precambrian shields, the high P-velocities (7.3 km/s) and intermediate Poisson's ratios (0.26–0.27) fall within the field of metapelites (Fig. 1-10). An alternative interpretation, however, would be a mixture of high-σ mafic granulites and low-σ pyroxenites (bronzite, for example, has a low Poisson's ratio of 0.21; Christensen and Fountain, 1975). The intermediate P-velocity (6.9 km/s) and high Poisson's ratio (0.28–0.29) determined for the Basin and Range are consistent with mafic granulite, anorthosite, or amphibolite, or a mixture of these rock types. In the Paleozoic of Southwest Germany, the measured P-velocities and Poisson's ratios vary from values appropriate for felsic to intermediate granulites (V_p = 6.4 km/s, σ = 0.25) to values indicative of a mix of intermediate and mafic granulites (V_p = 6.7 km/s, σ = 0.28).

Of course, these conclusions must be viewed with the proper caution. So far, very few shear-wave data have been interpreted, and in most existing studies the data are of marginal quality. Even more importantly, we must remember that determinations of lithologies from seismic velocities generally refer to the average composition of an entire lower-crustal block measuring tens of kilometers across and 10–20 km thick. Yet we know from multichannel seismic reflection data and high-grade metamorphic terrains that the deep crust must be heterogeneous on the scale of tens to hundreds of meters (e.g., Fountain and Salisbury, 1981). Thus, a lower crust whose seismic properties are compatible with a bulk composition of intermediate granulite probably contains significant amounts of more felsic and more mafic rocks. Improving the resolution with which the physical properties of the lower crust can be determined remains one of the challenges of deep crustal seismology.

5. Fluids and anisotropy

The conclusions about deep crustal composition we have drawn above depend on the key assumptions that the deep continental crust is isotropic and free of fluids. Because these assumptions are inevitably idealizations of an imperfect Earth, we must ask ourselves (1) how anisotropic is the Earth's crust? and (2) how prevalent are pore fluids in the deep crust? The answers to these questions will undoubtedly change from place to place, and perhaps from experiment to experiment, as seismic source characteristics change.

The primary evidence for fluids in the deep continental crust comes from interpretations of electromagnetic data, which in many places (particularly in Phanerozoic crust) require a zone of high conductance in the lower crust (Hyndman and Hyndman, 1968; Shankland and Ander, 1983; Jones, 1987). Saline fluids in rocks with a few per cent porosity would account for the high conductivity (Hyndman and Shearer, 1989). The effect that such porosity would have on seismic velocities depends on the pore pressure of the fluid: fluids at low pore pressure will have a negligible effect on seismic velocity, while pore pressures increasing to near-lithostatic will have a drastic effect on velocity (Todd and Simmons, 1972; Christensen, 1984). For the low-porosity metamorphic and igneous rocks expected in the lower crust, porosity of several per cent would have to be held open by high pore pressure.

If saturated pore spaces are indeed widespread in the lower crust, the estimates of bulk composition inferred from seismic velocities will be biased toward felsic compositions, as pointed out by Hyndman and Klemperer (1989). Our estimates of composition, which assume a dry crust, could therefore be considered a felsic end-member of the possible bulk composition. Shear-wave data offer a potential means of detecting zones of fluid-filled porosity, because the presence of fluids at high pore pressure increases Poisson's ratio (Christensen, 1984). Fluid-filled cracks have also been proposed as a mechanism for generating lower-crustal reflections (Matthews and Cheadle, 1986; Hyndman, 1988; Hyndman and Shearer, 1989); however, this mechanism is difficult to reconcile with the weak amplitudes of shear-wave reflections corresponding to the lower-crustal P-wave reflections (Holbrook et al., 1987, 1988; Goodwin and McCarthy, 1990).

The existence of seismic anisotropy in the lower continental crust remains an open question. Seismic anisotropy has been measured in the oceanic and continental upper mantle (Raitt et al., 1969; Bamford, 1977; Fuchs, 1983) and in the upper crust (e.g., Crampin et al., 1984), but no conclusive measurements of lower-crustal anisotropy have been made. This is somewhat surprising, because laboratory measurements of P-velocities (Table 1-3) show that several lower-crustal rock types have significant anisotropy, particularly quartz-mica schists (10.7%), felsic amphibolite gneiss (7.3%), granulite-facies metapelite (5.5%), and amphibolite (5.4%). Moreover, the horizontally layered lower crust seen in many multichannel reflection sections (e.g., Brown et al., 1986) should produce transverse isotropy (Crampin, 1989), a particular kind of anisotropy in which the horizontal velocity is constant in all directions, but the horizontal and vertical velocities differ. Such anisotropy in the lower crust would be expected to produce shear-wave splitting of the Moho reflection, S_mS; unfortunately, few wide-angle, three-component seismic studies have been carried out, and existing studies have not detected significant splitting of S_mS (e.g., Gajewski and Prodehl, 1987; Holbrook et al., 1988). Furthermore, shear-wave splitting observed on earthquake records in Japan has been interpreted as the result of anisotropy in the upper, not the lower, crust (Kaneshima and Ando, 1989). On the basis of present data, then, we must conclude at present that either the lower crust is isotropic, or that anisotropy exists in isolated blocks whose size lies beneath the resolution of current experiments. Nevertheless, seismic anisotropy is an important property of crustal samples recovered from outcrops and drill holes, and probably influences crustal reflectivity (e.g., Jones and Nur, 1982, 1984; Christensen and Szymanski, 1988; Christensen, 1989; Fountain et al., 1990).

6. Discussion

6.1. Average continental crustal structure

Our compilation of field-measured seismic velocities allows the construction of some generalized models of deep crustal structure as a function of tectonic environment. Although such models run the risk of oversimplification, they can provide useful characterizations of the seismic structure of the continental crust. Using the data from Table 1-2, we can construct a standard crustal column for each tectonic environment, showing (1) average thicknesses of the crust, middle crust, and lower crust, and (2) modal velocities of the deep crust (Fig. 1-11). These columns show that the crust is thickest beneath continent–continent collision zones, shields, and platforms, while the crust is thinnest beneath passive margins, forearcs, and rifts. In general, a three-layer crust, with velocities increasing with depth, is a useful model; in most tectonic environments, the middle and lower crust together comprise about 2/3 of the total crust.

We have constructed from these crustal columns a generalized cross-section through a hypothetical continent bounded by an active and a passive margin (Fig. 1-12). This cartoon depicts the general velocity structure of the continental crust across some common tectonic environments: clearly shown, for example, is the bimodal distribution of lower-crustal velocities (6.7–6.8 and 7.1–7.3 km/s) and the predominance of mid-crustal velocities in the range 6.4–6.7 km/s.

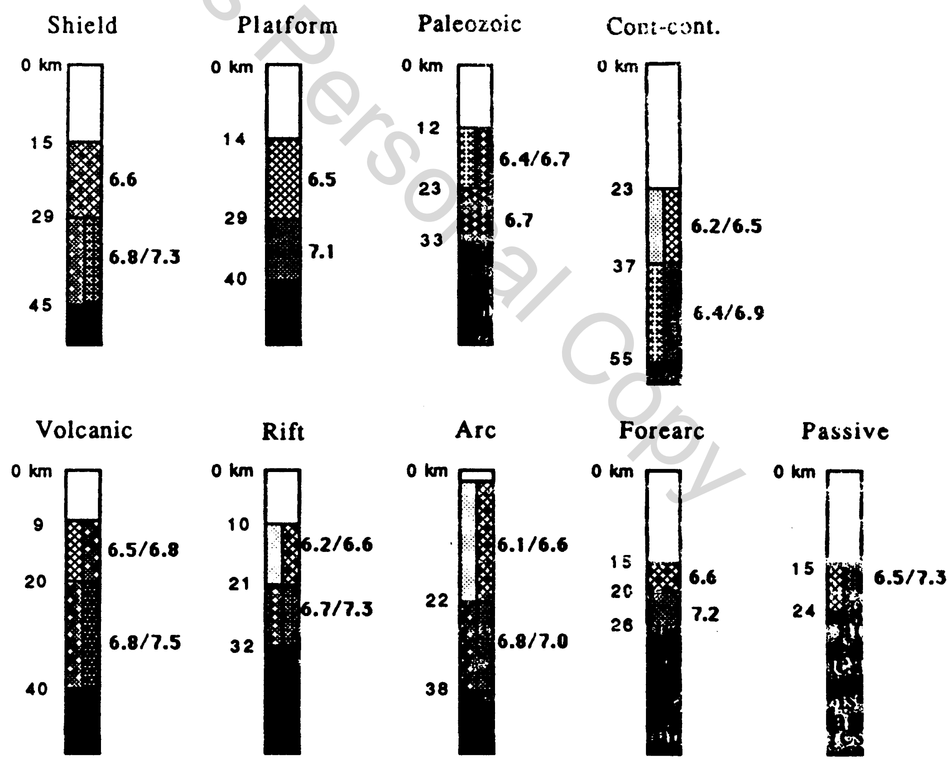

Fig. 1-11. Summary of average crustal columns in various tectonic environments, showing average thickness of crustal layers and modal velocities, determined from histograms of Fig. 1-8. Shading indicates velocity values; split layers indicate bimodal velocity distributions. Black represents upper mantle. The crust is thickest beneath continent–continent collision zones, shields, platforms, and volcanic plateaus, while it is thinnest beneath passive margins, forearcs, and rifts

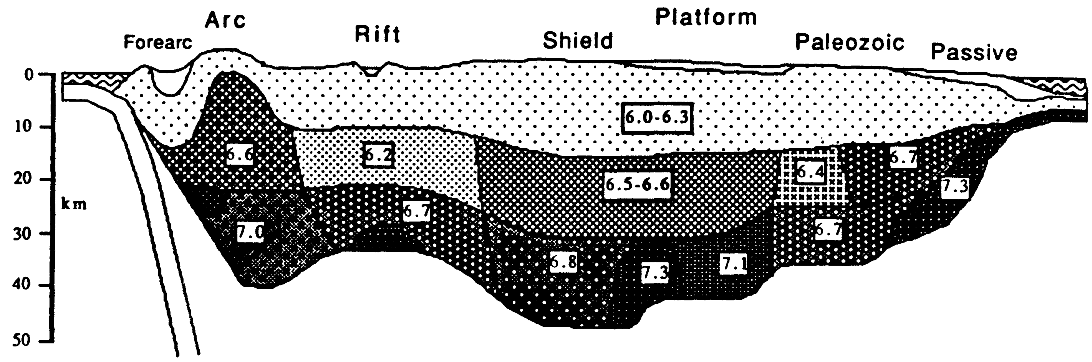

Fig. 1-12. Cartoon cross-section across a hypothetical continent, showing average seismic properties in various tectonic provinces. The velocity in the upper crust is assumed to be 6.0–6.3 km/s everywhere. Note the strong lateral changes in crustal structure from province to province. High-velocity (7.1–7.3 km/s) layers are found beneath rifts, shields, platforms, and passive margins. Mid-crustal velocities are lowest beneath rifts, perhaps due to higher temperatures.

6.2. Bulk lower-crustal composition

The bulk composition of the continental crust has long been under debate, yet is still poorly known. The primary reason for this uncertainty is the difficulty in estimating the composition of the deep crust. Geological estimates of lower-crustal composition derived from studies of Precambrian granulite terrains (e.g., Weaver and Tarney, 1984; Shaw et al., 1986), island arcs (Taylor and McLennan, 1981), and xenoliths (e.g., Dupuy et al., 1979) generally fall in the range 54–61% SiO_2, corresponding to an intermediate (dioritic) composition.

Smithson and his coworkers (Smithson and Brown, 1977; Smithson, 1978; Smithson et al., 1981), using measurements of mean crustal velocity and observations from multichannel reflection data, also inferred a dioritic (59% SiO_2) lower-crustal composition. According to Smithson and Brown (1977), "the lower crust must be distinctly less mafic... than gabbro." This conclusion was based on (1) their observation that most lower crustal P-velocities are less than 7.0 km/s, corresponding to the range of felsic and intermediate granulites, and (2) the existence of numerous reflections in the lower crust on multichannel reflection profiles, thus implying the presence of more felsic (i.e., lower-velocity) rocks.

Our summary of seismic velocities has an important bearing on such estimates of bulk lower-crustal composition. For this purpose, however, the velocity histograms of Figures 1-5 and 1-6 are somewhat misleading, in that some tectonic provinces have been over- or under-sampled with respect to their global volumetric abundance. In order correct for this sampling bias, we applied a weighting factor to each velocity determination, based on the ratio of the proportion of total crustal area measured in each tectonic environment to the approximate global volumetric abundance of crust in that environment (Table 1-6). The weighting factors thus calculated show that, relative to their global volumetric abundance, shields, volcanic plateaus, and rifts have been oversampled, while platforms, forearcs, and passive margins have been undersampled by seismic experiments.

The resulting corrected velocity histograms, shown in Figure 1-13, show several important differences to the uncorrected histograms (Figs. 1-5 and 1-6), especially in the lower crust (Fig. 1-13b). Particularly obvious is the marked increase in the proportion of velocities in the range 7.0–7.2 km/s; this is primarily due to the increasing contribution of platforms, which have a strong velocity peak in that range (Fig. 1-8b). There has been a relative

TABLE 1-6

Calculation of weighting factors for velocity histogram correction

Tectonic environment[1]	Area surveyed[2]		% of total area surveyed[3]		Vol.% worldwide[4]	Weighting factor[5]	
	lower	middle	lower	middle		lower	middle
Shield	129.0	93.4	35.4	35.1	15	0.4	0.4
Platform	48.4	45.7	13.3	17.2	40	3.0	2.3
Paleozoic	47.1	40.7	12.9	15.3	16	1.2	1.0
Cont. collision	46.0	30.3	12.6	11.2	16	1.3	1.4
Volcanic plat.	16.5	9.6	4.5	3.6	[1]	0.2	0.3
Rift	49.9	34.1	13.7	12.8	1	0.1	0.1
Arc	16.0	9.8	4.4	3.7	4	0.9	1.1
Forearc	3.3	2.2	0.9	0.8	[2]	2.2	2.5
Passive margin	7.9	0.3	2.2	0.1	[5]	2.3	10.0

[1] Tectonic environment;

[2] Total cross-sectional area of middle and lower crust surveyed by wide-angle seismic experiments;

[3] Area surveyed as a percentage of total area surveyed;

[4] Estimated global volumetric abundance, expressed as percent of total continental crust, taken from Condie (1982) except where denoted by brackets;

[5] Weighting factors to correct for bias in distribution of wide-angle seismic surveys, calculated from the ratio of percentage of worldwide volume to percentage of total area surveyed.

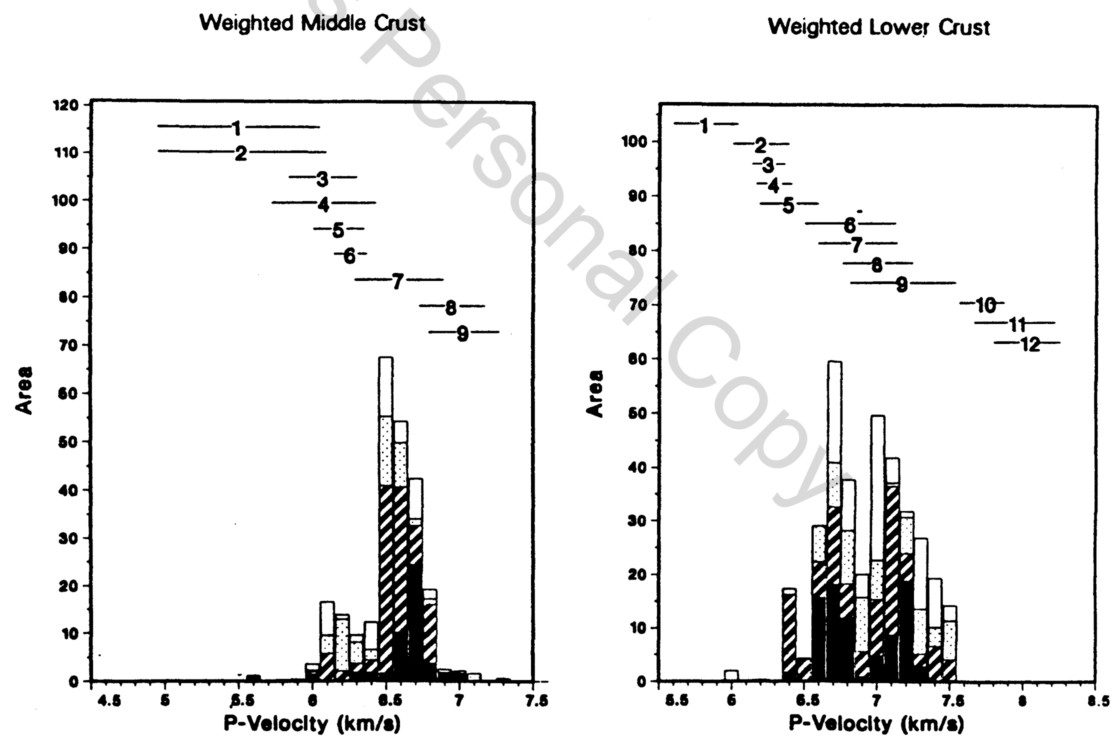

Fig. 1-13. Velocity histograms for the (a) middle crust and (b) lower crust, calculated from the histograms of Figs. 1-5 and 1-6 but using the weighting factors of Table 1-6. These weighted histograms more accurately reflect the average properties of the middle and lower crust, because over- and undersampling of some tectonic provinces has been approximately corrected for. Shading indicates quality factor (see Fig. 1-5). Bars at top show velocity ranges of possible (a) mid-crustal and (b) lower-crustal rocks (see Table 1-3 and Figs. 1-5 and 1-6).

decrease in the proportion of velocities in the range 7.3–7.5 km/s, especially among the better-determined values; this is due to the decreased contribution of shields, rifts, and volcanic plateaus, all of which show high-velocity peaks. As a result, the bimodal nature of the lower-crustal velocity distribution has been enhanced, with 64% of the total area (72% of the best-determined values) falling within the ranges 6.7–6.8 km/s and 7.0–7.2 km/s. This is a remarkable observation, as it implies that about 2/3 of the lower continental crust worldwide has an average P-velocity within those relatively narrow ranges.

If the weighted lower-crustal velocity histogram is approximately correct, it implies that roughly half (53%) of the lower continental crust has a velocity of 7.0 km/s or greater. Smithson's (1978) estimate of the average velocity of the lower crust was therefore low, due to the smaller refraction data base available to him. Moreover, many lower-velocity regions (6.7–6.8 km/s) may consist of predominantly mafic material, since the temperature-corrected velocities of many mafic granulites fall within that range (6.86 ± 0.27 km/s, Table 1-3). These two observations suggest that the composition of the lower crust in many places is closer to gabbroic than to the dioritic compositions derived by Smithson (1978), or from geologic and geochemical data by Taylor and McLennan (1981), Weaver and Tarney (1984), and Shaw et al. (1986). This conclusion would concur with the review of xenolith evidence (Griffin and O'Reilly, 1987; Rudnick, this volume), which suggests that mafic rocks are far more prevalent in the lower crust than felsic or intermediate rocks. An alternative explanation for the high velocities would be the presence of garnet, which would allow more felsic compositions, if significant amounts of metapelite are present.

There is, of course, some danger in overinterpreting summary diagrams such as those in Figure 1-13: as we have seen, the seismic characteristics of the deep continental crust vary markedly from place to place, even within similar tectonic environments. The most reliable estimates of lower-crustal composition will be those at individual, well-studied locations, where a combination of geophysical and geological data exists.

6.3. Constraints from seismic reflection profiling

The results of deep seismic reflection profiles provide additional constraints on conclusions regarding the composition and physical properties of the crust. Although seismic reflection data provide structural resolution unavailable from refraction methods, they do not provide accurate deep velocity information, due to their limited aperture (usually <10 km). The primary observation from reflection profiles that we address here is the high reflectivity of the lower crust, often with a well-defined top and bottom to the reflective zone (e.g., Mooney and Brocher, 1987). Unfortunately, any comparison of seismic reflection results with wide-angle reflection/refraction results is made difficult by the dissimilar coverage currently available for the two methods. For example, we noted above that wide-angle seismic data have been extensively recorded within shields and platforms, but these regions are sparsely sampled by reflection profiles, which are biased toward continental margins and regions of relatively thin (≤35 km) crust. Despite the differences in coverage, the following conclusions can be drawn.

Although lower crustal reflectivity varies significantly from region to region, it is generally quite high in rifts and areas of extended crust (e.g., McCarthy and Thompson, 1988). The wide-angle seismic results presented here show that these areas have high Poisson's ratio, indicative of a mafic lower crust. This inferred composition is consistent with the suggestion that crustal reflectivity in these areas is in part due to mafic intrusions. Alternatively, ductile shear in extended lower crust would result in the alignment of anisotropic minerals with the higher P-wave axis horizontal; anastomozing shear zones could produce high lower crustal reflectivity without requiring numerous mafic intrusions (Jones and Nur, 1984). The high velocity layers (7.2–7.5 km/s) found beneath some rifts and passive margins likely consist of a mix of mafic and ultramafic rocks. If layered, this zone would be highly reflective, consistent with a clearly defined "reflection Moho" in extended regions (e.g., Klemperer et al., 1986; McCarthy and Thompson, 1988).

The origin of lower crustal reflectivity remains a major unknown. Because deep reflections originate from boundaries separating layers of contrasting seismic impedance (velocity x density), they must hold important clues for improving our knowledge of deep crustal composition. Several origins have been proposed for deep crustal reflections, including compositional layering (igneous or metamorphic layering; Hale and Thompson, 1982; Christensen, 1989), ductile shear zones (Jones and Nur, 1982, 1984), igneous intrusions (Meissner, 1973), lenses of partial melt (Meissner, 1973; Hale and Thompson, 1982), and the presence of fluid-filled cracks (Matthews and Cheadle, 1986). The wide range of lower-crustal velocities compiled above, which implies a large diversity in rock types in the lower crust, suggests that no single cause is responsible for all deep reflections. Although we are unable to determine the causes of deep reflections with our compilation, there is clearly a need to make detailed comparisons of reflection and refraction results at locations where both types of data exist (e.g., Bartelsen et al., 1982; Wever, 1989). Coincident shear-wave data can be particularly illuminating in constraining the origin of deep reflections (e.g., Holbrook et al., 1988).

6.4. Implications for crustal evolution

Models of the growth of continental crust through time vary widely, but most suggest that the bulk of continental crust was produced during the Archean, by about 2.5 Ga (e.g., McLennan and Taylor, 1982; Reymer and Schubert, 1984). The widespread Archean granite-greenstone belts were created by the melting of mafic source rocks (Rudnick and Taylor, 1986), probably in intra-arc (Sleep and Windley, 1982) or intracontinental rift (Kröner, 1984) settings. During the Phanerozoic, in contrast, accretion of continental crust took place primarily by arc magmatism (e.g., Hamilton, 1981, 1988), with contributions from rift and hotspot magmatism. In tackling the problem of crustal evolution from a seismological standpoint, then, we must examine two kinds of tectonic environments: stable cratons and regions of more recent magmatic activity, such as arcs, rifts and volcanic plateaus.

A widely used model for the growth of the continental crust at magmatic arcs during the Phanerozoic is the andesite model of Taylor (1977). This model, which assumes additions to the crust of bulk andesitic composition, uses a mass balance to predict a mafic composition for the lower crust (e.g., Taylor and McLennan, 1981). Since the work of Smithson (1978), many authors (e.g., Kay and Kay, 1986) have pointed out an apparent contradiction between the mafic lower crust required by the andesite model and the intermediate lower crust proposed by Smithson (1978) on the basis of P-wave velocities. As pointed out above, however, our compilation shows that in most tectonic environments, *in situ* lower crustal compressional velocities are indeed compatible with mafic compositions (Table 1-5). The limited seismic information from arcs themselves show velocities of 6.7–6.8 km/s in island arcs (Asano et al., 1985; Iwasaki et al., 1990) and 6.9–7.0 km/s in Andean-type arcs (Pakiser and Brune, 1980; Leaver et al., 1984); these values are all consistent with mafic granulites (6.86 ± 0.27 km/s; Table 1-3). There is thus no need to appeal to alternative explanations such as the presence of fluid-filled cracks (Hyndman and Klemperer, 1989), widespread hydrous minerals, or foundering of mafic rocks into the mantle to reconcile the seismic and geologic evidence.

The bimodal distribution of P-velocities beneath shields and platforms (Fig. 1-8a,b) suggests that two distinct crust-forming processes may have been active during the Precambrian. The similarity between the low-velocity peak (6.6–6.8 km/s) and the values found beneath arcs (Fig. 1-8g) suggests that the lower crust beneath some shields and platforms was formed by arc magmatism. This interpretation is consistent with most models of Precambrian crustal evolution, which generally assert that modern-style subduction zones have existed since the Archean (e.g., Tarney and Windley, 1977; Windley, 1981) or Proterozoic (e.g., Hargraves, 1981). The high-velocity peak (7.1–7.5 km/s), on the other hand, can be explained either as the result of the underplating of mafic and ultramafic magmas (e.g., Furlong and Fountain, 1986) or the presence of high-grade metamorphic rocks of supracrustal origin (metapelites). The interpretation of underplated material at the base of cratons is consistent with models of early Precambrian crustal evolution, which envision continental growth by underplating of magmas from a vigorously convecting mantle (e.g., Kröner, 1981). Alternatively, the high P-velocities could be the result of a prevalence of garnetiferous metapelites, which may have been accreted to the base of the crust in Precambrian orogenic belts. This process must have occurred to some extent during the Archean, as evidenced by the existence of granulite-facies metapelites in some Archean terrains (e.g., Fountain and Salisbury, 1981).

The activity of mafic/ultramafic underplating during the Phanerozoic is indicated by the presence of high seismic velocities (7.1–7.5 km/s) beneath many rifts, volcanic plateaus, and passive margins (Fig. 1-8). This process has been suggested to occur beneath volcanic plateaus and at rifted continental margins where a mantle thermal anomaly exists (White et al., 1987; White and McKenzie, 1989). The high velocities are predicted by thermal and petrologic considerations (Furlong and Fountain, 1986; White and McKenzie, 1989). Thus magmatic underplating appears to supplement arc magmatism as an important means of continental growth during the Phanerozoic.

6.5. Directions for future research

Our knowledge of the evolution of the lower continental crust is severely hampered by the paucity of high-quality data in several key tectonic environments, especially island arcs, Andean-type arcs, and continent–continent collision zones. These regions typically present logistical obstacles to the collection of wide-angle data, but these must be overcome if we are to understand the influence of these areas on crustal evolution.

A further important development will be the increased use of shear-wave information in wide-angle seismic experiments. Crustal seismologists must free themselves of the pervasive bias toward P-waves: even if techniques are developed which greatly improve resolution, P-wave velocity alone will always give an incomplete picture of the lower crust, due to the inescapable overlap of the P-velocities of diverse rock types (e.g., Table 1-2). Shear-wave information helps overcome this ambiguity.

There is a vital need for field and laboratory measurements addressing the two fundamental assumptions of this study: the lack of (1) anisotropy and (2) fluids in deep crust. Studies of *in situ* anisotropy in the Earth have focused on the upper crust and the oceanic and continental upper mantle; very little work has been done, however, on the anisotropy of the lower crust, despite the fact that many metamorphic rock types expected to exist in the lower crust show considerable anisotropy in the laboratory (Table 1-3). The role of fluids in the deep crust is still under debate (e.g., Fyfe et al., 1978; Shankland and Ander, 1983; Hall, 1986; Hyndman and Klemperer, 1989), but little is known about the influence of fluids on seismic velocities at pressures and temperatures appropriate for the lower crust.

7. Conclusions

The summary of deep crustal velocities presented here is, first and foremost, testimony to the diversity of the deep continental crust. The wide range of P-velocities found in the middle crust (6.0–7.1 km/s) and lower crust (6.4–7.5 km/s) implies the existence of bulk compositions varying, from place to place, from felsic to mafic/ultramafic. Still, some generalizations can be made: most mid-crustal P-velocities fall in the range 6.5–6.8 km/s, while most in the lower crust lie in the ranges 6.7–6.8 km/s or 7.0–7.2 km/s. Lower-crustal velocities have a bimodal distribution beneath shields, platforms, passive margins, rifts, and volcanic plateaus, suggesting the influence of either mafic/ultramafic magmatic activity or high-grade metamorphism to raise P-velocities.

Inferences about composition drawn from P-velocities are non-unique, but this ambiguity can be significantly reduced by the existence of complementary S-velocity (and hence Poisson's ratio) information. The sparse shear-wave information available for the lower crust suggests that S-velocities are relatively high beneath shields and platforms (i.e. Poisson's ratio is low), supporting the presence of either quartz-rich metapelites or low-σ pyroxene. The bimodal pattern may be the manifestation of two distinct processes of Precambrian crustal genesis: mafic/ultramafic underplating and arc magmatism. P-velocities beneath most Phanerozoic environments fall in the range 6.6–6.8 km/s, consistent with a predominantly mafic bulk composition; this interpretation is in accord with a model of crustal growth by arc magmatism. The presence of high velocities (7.1–7.5 km/s) beneath Phanerozoic rifts, volcanic plateaus, and passive margins is likely the result of mafic/ultramafic underplating in those regions.

Finally, our compilation shows that high velocities ($\geq$7.0 km/s) are more common in the lower crust than previously thought. In most tectonic environments, P-wave velocities are consistent with a bulk mafic lower crust. This conclusion eliminates the often-quoted paradox between estimates of bulk lower-crustal composition from seismic methods and geologic evidence.

Acknowledgments

We thank David Fountain and Roy Johnson for thorough, constructive reviews. Support for W.S.H. was provided by a Woods Hole Oceanographic Institution Postdoctoral Scholarship.

References

Asano, S. and 10 others, 1985. Crustal structure in the northern part of the Philippine Sea Plate as derived from seismic observations of Hatoyama off Izu Peninsula explosions. J. Phys. Earth, 33: 173–189.

Assumpçao, M. and Bamford, D., 1978. LISPB — V. Studies of crustal shear waves. Geophys. J. R. Astron. Soc., 54: 61–73.

Avedik, F., Berendsen, D., Fucke, H., Goldflam, S., Hirschleber, H., Meissner, R., Sellevoll, M.A. and Weinrebe, W., 1984. Seismic investigations along the Scandinavian "Blue Norma" profile. Ann. Geophys., 2: 571–578.

Azbel, I.Y., Buyanov, A.F., Ionkis, V.T., Sharov, N.V. and Sharova, V.P., 1989. Crustal structure of the Kola Peninsula from inversion of deep seismic sounding data. Tectonophysics, 162: 87–99.

Babuska, V., 1972. Elasticity and anisotropy of dunite and bronzitite. J. Geophys. Res., 77: 6955–6965.

Bamford, D., 1977. Pn velocity anisotropy in a continental upper mantle. Geophys. J. R. Astron. Soc., 49: 29–48.

Bamford, D., Nunn, K., Prodehl, C. and Jacob, B., 1978. LISPB — IV. Crustal structure of northern Britain. Geophys. J. R. Astron. Soc., 54: 43–60.

Banda, E. and Ansorge, J., 1980. Crustal structure under the central and eastern part of the Betic Cordillera. Geophys. J. R. Astron. Soc., 63: 515–532.

Banda, E., Suriñach, E., Aparicio, A., Sierra, J. and Ruiz de la Parte, E., 1981. Crust and upper mantle structure of the central Iberian Meseta (Spain). Geophys. J. R. Astron. Soc., 67: 779–789.

Barazangi, M. and Brown, L. (Editors), 1986a. Reflection Seismology: A Global Perspective. American Geophysical Union, Geodynamics Series 13, Washington, D.C., 311 pp.

Barazangi, M. and Brown, L. (Editors), 1986b. Reflection Seismology: A Global Perspective. American Geophysical Union, Geodynamics Series 14, Washington, D.C., 339 pp.

Bartelsen, H., Lüschen, E., Krey, T., Meissner, R., Schmoll, H. and Walter, C., 1982. The combined seismic reflection-refraction investigation of the Urach geothermal anomaly. In: R. Haenel (Editor), The Urach Geothermal Project. Schweizerbart'sche Verlag, Stuttgart, pp. 247–262.

Barton, P.J. and Matthews, D.H., 1984. Deep structure and geology of the North Sea region interpreted from a seismic refraction profile. Ann. Geophys., 2: 663–668.

Beaudoin, B., 1989. Crustal structure of the Yukon-Tanana terrane along the TACT corridor: Evidence for lower crustal detachment. EOS, Trans. AGU, 70: 1337.

Berry, M.J., 1973. Structure of the crust and upper mantle in Canada. Tectonophysics, 20: 183–201.

Birch, F., 1960. The velocity of compressional waves in rocks to 10 kilobars, Part 1. J. Geophys. Res., 65: 1083–1102.

Birch, F., 1961. The velocity of compressional waves in rocks to 10 kilobars, Part 2. J. Geophys. Res, 66: 2199–2224.

Blümling, P., Mooney, W.D. and Lee, W.H.K., 1985. Crustal structure of the Calaveras Fault zone, central California, from seismic refraction investigations. Bull. Seismol. Soc. Am., 75: 193–209.

Boland, A.V. and Ellis, R.M., 1989. Velocity structure of the Kapuskasing uplift, northern Ontario, from seismic refraction studies. J. Geophys. Res., 94: 7189–7204.

Boland, A.V. and Ellis, R.M., 1991. A geophysical model for the Kapuskasing Uplift from seismic and gravity studies. Can. J. Earth Sci., 28: 342–354.

Bonatti, E. and Seyler, M., 1987. Crustal underplating and evolution in the Red Sea Rift: Uplifted gabbro/gneiss complexes of Zabargad and Brothers Islands. J. Geophys. Res., 92: 12,803–12,821.

Bonner, B.P. and Schock, R.N., 1981. Seismic wave velocity. In: W. R. Judd and R.F. Roy (Editors), Physical Properties of Rocks and Minerals. McGraw-Hill, McGraw-Hill/CINDAS Data Series on Material Properties II-2, pp. 221–256.

Braile, L.W., Smith, R.B., Keller, G.R. and Welch, R.M., 1974. Crustal structure across the Wasatch front from detailed seismic refraction studies. J. Geophys. Res., 79: 2669–2677.

Braile, L.W. and 9 others, 1982. The Yellowstone–Snake River Plain seismic profiling experiment: crustal structure of the eastern Snake River Plain. J. Geophys. Res., 87: 2597–2609.

Brown, L., Barazangi, M., Kaufman, S. and Oliver, J., 1986. The first decade of COCORP: 1974–1984. In: M. Barazangi and L. Brown (Editors), Reflection Seismology: A Global Perspective. American Geophysical Union, Geodynamics Series 13, Washington, D.C., pp. 107–120.

Bullen, K.E. and Bolt, B.A., 1985. An Introduction to the Theory of Seismology. Cambridge University Press, Cambridge, U.K., 499 pp.

Catchings, R.D. and Mooney, W.D., 1988a. Crustal structure of the Columbia Plateau: evidence for continental rifting. J. Geophys. Res., 93: 459–474.

Catchings, R.D. and Mooney, W.D., 1988b. Crustal structure of East Central Oregon: relation between Newberry Volcano and regional crustal structure. J. Geophys. Res., 93: 10,081–10,094.

Catchings, R.D. and Mooney, W.D., 1990. Basin and Range crustal and upper mantle structure along the 40°N parallel, northwest Nevada. J. Geophys. Res., in review.

Cerveny, V., Molotkov, I.A. and Psencik, I., 1977. Ray Method in Seismology. University of Karlova, Prague, 214 pp.

Christensen, N.I., 1965. Compressional wave velocities in metamorphic rocks at pressures to 10 kilobars. J. Geophys. Res., 70: 6147–6164.

Christensen, N.I., 1966a. Shear wave velocities in metamorphic rocks at pressures to 10 kilobars. J. Geophys. Res., 71: 3549–3556.

Christensen, N.I., 1966b. Elasticity of ultrabasic rocks. J. Geophys. Res., 71: 5921–5931.

Christensen, N.I., 1972. The abundance of serpentinites in the oceanic crust. J. Geol., 80: 709–719.

Christensen, N.I., 1977. The geophysical significance of oceanic plagiogranite. Earth Planet. Sci. Lett., 36: 297–300.

Christensen, N.I., 1978. Ophiolites, seismic velocities and oceanic crustal structure. Tectonophysics, 47: 131–157.

Christensen, N.I., 1979. Compressional wave velocities in rocks at high temperature and pressures, critical thermal gradients and crustal low-velocity zones. J. Geophys. Res., 84: 6849–6857.

Christensen, N.I., 1982. Seismic velocities. In: R. S. Carmichael (Editors, Handbook of Physical Properties of Rocks, 2. CRC Press, Boca Raton, Fla., pp. 1–228.

Christensen, N.I., 1984. Pore pressure and oceanic crustal seismic structure. Geophys. J. R. Astron. Soc., 79: 411–423.

Christensen, N.I., 1989. Reflectivity and seismic properties of the deep continental crust. J. Geophys. Res., 94: 17,793–17,804.

Christensen, N.I. and Fountain, D.M., 1975. Constitution of the lower continental crust based on experimental studies of seismic velocities in granulite. Geol. Soc. Am. Bull., 86: 227–236.

Christensen, N.I. and Szymanski, D.L., 1988. Origin of reflections from the Brevard fault zone. J. Geophys. Res, 93: 1087–1102.

Christensen, N.I. and Wepfer, W.W., 1989. Laboratory techniques for determining seismic velocities and attenuations, with applications to the continental lithosphere. In: L. C. Pakiser and W.D. Mooney (Editors), The Geophysical Framework of the Continental United States. Geol. Soc. Am., Mem., 172: 91–102.

Christensen, N.I., Carlson, R.L., Salisbury, M.H. and Fountain, D.M., 1975. Elastic wave velocities in volcanic and plutonic rocks recovered on DSDP Leg 31. In: Initial Reports of the DSDP, 31: 607–610.

Chroston, P.N. and Brooks, S.G., 1989. Lower crustal seismic velocities from Lofoten-Vesteralen, N. Norway. Tectonophysics, 157: 251–269.

Chroston, P.N. and Evans, C.J., 1983. Seismic velocities of granulites from the Seiland petrographic province, N. Norway. J. Geophys., 52: 14–21.

Clowes, R.M., Gens-Lenartowicz, E., Demartin, M. and Saxov, S., 1987. Lithospheric structure in southern Sweden –results from FENNOLORA. Tectonophysics, 142: 1–14.

Colburn, R.H. and Mooney, W.D., 1986. Two-dimensional velocity structure along the synclinal axis of the Great Valley, California. Bull. Seismol. Soc. Am., 76: 1305–1322.

Condie, K.C., 1982. Plate Tectonics and Crustal Evolution. Pergamon Press, Oxford, 310 pp.

Conrad, V., 1925. Laufzeitkurven des Tauernbebens vom 28. November 1923. Mitt. Erdb. Komm. Wiener Akad. Wiss., 59: 1–23.

Crampin, S., Chesnokov, E.M. and Hipkin, R.G., 1984. Seismic anisotropy –the state of the art: II. Geophys. J. R. Astron. Soc., 76: 1–16.

Crampin, S., 1989. Suggestions for a consistent terminology for seismic anisotropy. Geophys. Prospect., 37: 753–770.

Cumming, W.B., Clowes, R.M. and Ellis, R.M., 1979. Crustal structure from a seismic refraction profile across southern British Columbia. Can. J. Earth Sci., 16: 1024–1040.

Davydova, N.I., Pavlenkova, N.E., Tulina, Yu.V. and Zverev, S.M., 1985. Crustal structure of the Barents Sea from seismic data. Tectonophysics, 114: 213–231.

Deichmann, N., Ansorge, J. and Mueller, S., 1986. Crustal structure of the southern Alps beneath the intersection with the European Geotraverse. Tectonophysics, 126: 57–83.

Diebold, J.B. and Stoffa, P.L., 1981. The traveltime equation, tau-p mapping and inversion of common midpoint data. Geophysics, 46: 238–254.

Dupuy, C., Leyreloup, A. and Vernieres, J., 1979. The lower continental crust of the Massif Central (Bornac, France) –with special references to REE, U and Th composition, evolution and heat-flow production. Phys. Chem. Earth, 11: 401–415.

Egger, A., Demartin, M., Ansorge, J., Banda, E. and Maistrello, M., 1988. The gross structure of the crust under Corsica and Sardinia. Tectonophysics, 150: 363–389.

EUGENO-S, W.G., 1988. Crustal structure and tectonic evolution of the transition between the Baltic Shield and the North German Caledonides (the EUGENO-S Project). Tectonophysics, 150: 253–348.

Evans, C.J., 1980. The seismic velocities of the Ox Mountain granulites of Ireland and the implications for the interpretation of the crustal structure of north Britain. Geophys. J. R. Astron. Soc., 63: 417–426.

Finlayson, D.M., Collins, C.D.N. and Denham, D., 1980. Crustal structure under the Lachlan fold belt, southeastern Australia. Phys. Earth Planet. Inter., 21: 321–342.

Finlayson, D.M., 1982. Seismic crustal structure of the Proterozoic North Australian craton between Tennant Creek and Mount Isa. J. Geophys. Res., 87: 10,569–10,578.

Finlayson, D.M. and Ansorge, J., 1984. Workshop proceedings: Interpretation of seismic wave propagation in laterally heterogeneous structures. Report 258, Bureau of Mineral Resources, Geology and Geophysics, Australian Govt. Publishing Service, Canberra, A.C.T.

Finlayson, D.M. and Leven, J.H., 1987. Lithospheric structures and possible processes in eastern Australia from deep seismic investigations. Tectonophysics, 133: 199–215.

Finlayson, D.M., Collins, C.D.N. and Lock, J., 1984. P-wave velocity features of the lithosphere under the Eromanga Basin, eastern Australia, including a prominent mid-crustal (Conrad?) discontinuity. Tectonophysics, 101: 267–291.

Fountain, D.M., 1976. The Ivrea–Verbano and Strona–Ceneri zones, northern Italy: A cross-section of the continental crust –new evidence from seismic velocities of rock samples. Tectonophysics, 33: 145–165.

Fountain, D.M. and Christensen, N.I., 1989. Composition of the continental crust and upper mantle –a review. In: L. C. Pakiser and W.D. Mooney (Editors), Geophysical Framework of the Continental United States. Geol. Soc. Am., Mem., 172: 711–742.

Fountain, D.M. and Salisbury, M.H., 1981. Exposed cross-sections through the continental crust: Implications for crustal structure, petrology and evolution. Earth Planet. Sci. Lett., 56: 263–277.

Fountain, D.M., Salisbury, M.H. and Percival, J., 1990. Seismic structure of the continental crust based on rock velocity measurements from the Kapuskasing Uplift. J. Geophys. Res., 95: 1167–1186.

Fox, P.J., Schreiber, E. and Peterson, J.J., 1973. The geology of the ocean crust: Compressional wave velocities of oceanic rocks. J. Geophys. Res., 78: 5155.

Fuchs, K., 1983. Recently formed elastic anisotropy and petrological models for the continental subcrustal lithosphere in southern Germany. Phys. Earth Planet. Inter., 31: 93–118.

Fuchs, K. and Müller, G., 1971. Computation of synthetic seismograms with the reflectivity method and comparison with observations. Geophys. J. R. Astron. Soc., 23: 417–433.

Fuis, G.S., Mooney, W.D., Healy, J.H., McMechan, G.A. and Lutter, W.J., 1984. A seismic refraction survey of the Imperial Valley region, California. J. Geophys. Res., 89: 1165–1189.

Furlong, K.P. and Fountain, D.M., 1986. Continental crustal underplating: Thermal considerations and seismic-petrologic consequences. J. Geophys. Res., 91: 8285–8294.

Fyfe, W.S., Price, N.J. and Thompson, A.B., 1978. Fluids in the Earth's Crust. Elsevier, Amsterdam-New York, 383 pp.

Gajewski, D. and Prodehl, C., 1987. Seismic refraction investigation of the Black Forest. Tectonophysics, 142: 27–48.

Gajewski, D., Holbrook, W.S. and Prodehl, C., 1987. A three-dimensional crustal model of southwest Germany derived from seismic refraction data. Tectonophysics, 142: 49–70.

Gaulier, J.M., Le Pichon, X., Lyberis, N., Avedik, F., Geli, L., Moretti, I., Deschamps, A. and Hafez, S., 1988. Seismic study of the crust of the northern Red Sea and Gulf of Suez. Tectonophysics, 153: 55–88.

Ginzburg, A., Makris, J., Fuchs, K. and Prodehl, C., 1981. The structure of the crust and upper mantle in the Dead Sea Rift. Tectonophysics, 80: 109–119.

Ginzburg, A., Whitmarsh, R.B., Roberts, D.G., Montadert, L., Camus, A. and F. Avedik, 1985. The deep seismic structure of the northern continental margin of the Bay of Biscay. Ann. Geophys., 3: 499–510.

Gohl, K., Smithson, S.B. and Kristoffersen, Y., 1991. The structure of the Archean crust in SW Greenland from seismic wide-angle data: a preliminary analysis. In: R. Meissner, L. Brown, H.-J. Dürbaum, W. Franke, K. Fuchs and F. Seifert (Editors), Continental Lithosphere: Deep Seismic Reflections. Am. Geophys. Union, Geodynamics Series, 22: 53–57.

Goldflam, S., Hirschleber, H.B. and Janle, P., 1977. A refined crustal model and the isostatic state of the Scandinavian Blue Road area. J. Geophys., 42: 419–428.

Goodwin, E.B. and McCarthy, J., 1990. Composition of the lower crust, West-central Arizona transition zone, from vertical-incidence and wide-angle measurements of P and S. J. Geophys. Res., 95: 20,097–20,109.

Grad, M. and Luosto, U., 1987. Seismic models of the crust of the Baltic Shield along the SVEKA profile in Finland. Ann. Geophys., 5: 639–650.

Griffin, W.L. and O'Reilly, S.Y., 1987. The composition of the lower crust and the nature of the continental Moho — xenolith evidence. In: P.H. Nixon (Editor), Mantle Xenoliths. John Wiley and Sons, New York, N.Y., pp. 413–430.

Guterch, A., Grad, M. and Materzok, R., 1983. Structure of the earth's crust of the Permian Basin in Poland. Acta Geophys. Pol., 31: 121–138.

Hale, L.D. and Thompson, G.A., 1982. The seismic reflection character of the continental Mohorovičić discontinuity. J. Geophys. Res., 87: 4625–4635.

Hall, D.H. and Hajnal, Z., 1973. Deep seismic crustal studies in Manitoba. Bull. Seismol. Soc. Am., 63: 885–910.

Hall, J., 1986. The physical properties of layered rocks in the deep continental crust. In: J.B. Dawson, D.A. Carswell, J. Hall and K.H. Wedepohl (Editors), The Nature of the Lower Continental Crust. Geol. Soc. London, Geol. Soc. Spec. Publ., 24: 51–62.

Hall, J. and Simmons, G., 1979. Seismic velocities of Lewisian metamorphic rocks at pressures to 8 kilobars: Relationship to crustal layering in North Britain. Geophys. J. R. Astron. Soc., 58: 337–347.

Hamilton, W.B., 1981. Crustal evolution by arc magmatism. Philos. Trans. R. Soc. London, 301: 279–291.

Hamilton, W.B., 1988. Plate tectonics and island arcs. Bull. Geol. Soc. Am., 100: 1503–1527.

Hargraves, R.B., 1981. Precambrian tectonic style: A liberal uniformitarian interpretation. In: A. Kröner (Editor), Precambrian Plate Tectonics. Elsevier, Amsterdam, pp. 21–56.

Hennet, C.G., Luetgert, J.H. and Phinney, R.A., 1991. The crustal structure in central Maine from coherency processed refraction data. J. Geophys. Res., 96: 12,023–12,037.

Holbrook, W.S., 1988. Wide-angle seismic studies of crustal structure and composition in Nevada, California and Southwest Germany. Ph.D. thesis, Stanford University.

Holbrook, W.S., 1990. The crustal structure of the northwestern Basin and Range province, Nevada, from wide-angle seismic data. J. Geophys. Res., 95: 21,843–21,869.

Holbrook, W.S. and Mooney, W.D., 1987. The crustal structure of the axis of the Great Valley, California, from seismic refraction measurements. Tectonophysics, 140: 49–63.

Holbrook, W.S., Gajewski, D. and Prodehl, C., 1987. Shear-wave velocity and Poisson's ratio structure of the upper lithosphere in Southwest Germany. Geophys. Res. Lett., 14: 231–234.

Holbrook, W.S., Gajewski, D., Krammer, A. and Prodehl, C., 1988. An interpretation of wide-angle compressional and shear wave data in Southwest Germany: Poisson's ratio and petrological implications. J. Geophys. Res., 93: 12,081–12,106.

Howie, J. and Miller, K., 1988. Interpretation of coincident vertical-incidence and wide-angle seismic profiles across the central California margin. EOS, Trans. Am. Geophys. Union, 69: 1315.

Hyndman, R.D., 1988. Dipping seismic reflectors, electrically conductive zones and trapped water in the crust over a subducting plate. J. Geophys. Res., 93: 13,391–13,405.

Hyndman, R.D. and Hyndman, D.W., 1968. Water saturation and high electrical conductivity in the lower continental crust. Earth Planet. Sci. Lett., 4: 427–432.

Hyndman, R.D. and Klemperer, S.L., 1989. Lower-crustal porosity from electrical measurements and inferences about composition from seismic velocities. Geophys. Res. Lett., 16: 255–258.

Hyndman, R.D. and Shearer, P.M., 1989. Water in the lower continental crust: modelling magnetotelluric and seismic reflection results. Geophys. J. Int., 98: 343–365.

Ikami, A., Ito, K., Shibuya, K. and Kaminuma, K., 1985. Geophysical studies of crustal structure of the Ongul islands and the northern Mizuho Plateau, East Antarctica. Tectonophysics, 114: 371–387.

Iwasaki, T., Hirata, N., Kanazawa, T., Melles, J., Suyehiro, K., Urabe, T., Möller, L., Makris, J. and Shimamura, H., 1990. Crustal and upper mantle structure in the Ryukyu island arc deduced from deep seismic sounding. Geophys. J. Int., 102: 631–651.

Jackson, I. and Arculus, R.J., 1984. Laboratory wave velocity measurements on lower crustal xenoliths from Calcutteroo, South Australia. Tectonophysics, 101: 185–197.

Jacob, A.W.B., Kaminski, W., Murphy, T., Phillips, W.E.A. and Prodehl, C., 1985. A crustal model for a northeast–southwest profile through Ireland. Tectonophysics, 113: 75–103.

Jarchow, C.M. and Thompson, G.A., 1989. The nature of the Mohorovičić discontinuity. Annu. Rev. Earth Planet. Sci., 17: 475–506.

Jeffreys, H., 1926. On near earthquakes. Monthly Not. R. Astron. Soc. Geophys. Suppl., 1: 385.

Jentsch, M., 1979. Reinterpretation of a deep-seismic-sounding profile on the Ukrainian Shield. J. Geophys., 45: 355–372.

Jones, A.G., 1987. MT and reflection: an essential combination. Geophys. J. R. Astron. Soc., 89: 7–18.

Jones, T.D. and Nur, A., 1982. Seismic velocity and anisotropy in mylonites and the reflectivity of deep crustal faults. Geology, 10: 260–263.

Jones, T.D. and Nur, A., 1984. The nature of seismic reflections from deep crustal fault zones. J. Geophys. Res., 89: 3153–3171.

Kaila, K.L., 1986. Tectonic framework of Narmada–Son Lineament –a continental rift system in central India from deep seismic soundings. In: M. Barazangi and L. Brown (Editors), Reflection Seismology: A Global Perspective. American Geophysical Union, Geodynamics Series 13, Washington, D.C., 133–150.

Kaila, K.L., Krishna, V.G. and Mall, D.M., 1981. Crustal structure along Mehmadabad–Billimora profile in the Cambay Basin, India, from deep seismic soundings. Tectonophysics, 76: 99–130.

Kaila, K.L., Murty, P.R.K., Mall, D.M., Dixit, M.M. and Sarker, D., 1987. Deep seismic soundings along Hirnpur–Mandla profile, central India. Geophys. J. R. Astron. Soc., 89: 399–404.

Kaila, K.L.; Rao, I.B.P., Rao, P.K., Rao, N.M., Krishna, V.G. and Sridhar, A.R., 1989. DSS studies over Deccan Traps along the Thuadara–Sendhwa–Sindad profile, across Narmada–Son lineament, India. In: R. F. Mereu, S. Müller and D.M. Fountain (Editors), Properties and Processes of Earth's Lower Crust. Am. Geophys. Union, Monogr., 51: 121–125.

Kan, R.-J., Hu, H.-X., Zeng, R.-S., Mooney, W.D. and McEvilly, T.V., 1986. Crustal structure of Yunnan province, People's Republic of China, from seismic refraction profiles. Science, 234: 433–437.

Kanamori, H. and Mizutani, H., 1965. Ultrasonic measurements of elastic constants of rocks uner high pressures. Bull. Earthquake Res. Inst., 43: 173.

Kaneshima, S. and Ando, M., 1989. An analysis of split shear waves observed above crustal and uppermost mantle earthquakes beneath Shikoku, Japan: Implications in effective depth extent of seismic anisotropy. J. Geophys. Res., 94: 14,077–14,092.

Kay, R.W. and Kay, S.M., 1981. The nature of the lower continental crust: Inferences from geophysics, surface geology and crustal xenoliths. Rev. Geophys. Space Phys., 19: 271–297.

Kay, R.W. and S.M., Kay,, 1986. Petrology and geochemistry of the lower continental crust: an overview. In: J. B. Dawson, D.A. Carswell, J. Hall and K.H. Wedepohl (Editors), The Nature of the Lower Continental Crust. Geol. Soc. London, Geol. Soc. Spec. Publ., 24: 147–159.

Károly, P., István, A., Géza, R. and Géza, V., 1986. Characteristics of the reflecting layers in the earth's crust and upper mantle in Hungary. In: M. Barazangi and L. Brown (Editors), Reflection Seismology: A Global Perspective. American Geophysical Union, Geodynamics Series 13, Washington, D.C., pp. 55–65.

Keller, G.R., Smith, R.B. and Braile, L.W., 1975. Crustal structure along the Great Basin–Colorado Plateau transition from seismic refraction studies. J. Geophys. Res., 80: 1093–1098.

Kern, H., 1978. The effect of high temperature and high confining pressure on compressional wave velocities in quartz-bearing and quartz-free igneous and metamorphic rocks. Tectonophysics, 44: 185–203.

Kern, H., 1982. Elastic-wave velocity in crustal and mantle rocks at high pressure and temperature: The role of the high–low quartz transition and of dehydration reactions. Phys. Earth Planet. Inter., 29: 12–23.

Kern, H. and Schenk, V., 1985. Elastic wave velocities in rocks from a lower crustal section in southern Calabria (Italy). Phys. Earth Planet. Inter., 40: 147–160.

Kern, H. and Schenk, V., 1988. A model of velocity structure beneath Calabria, southern Italy, based on laboratory data. Earth Planet. Sci. Lett., 87: 325–337.

Klemperer, S.L., 1989. Deep seismic reflection profiling and the growth of the continental crust. Tectonophysics, 161: 233–244.

Klemperer, S.L., Hauge, T.A., Hauser, E.C., Oliver, J.E. and Potter, C.J., 1986. The Moho in the northern Basin and Range province, Nevada, along the 40°N seismic-reflection transect. Geol. Soc. Am. Bull., 97: 603–618.

Kondorskaya, N.V. and 10 others, 1981. Joint analysis of seismological data by the USSO and DSS stations in the Caucasus region. Pure Appl. Geophys., 119: 1167–1179.

Kroenke, I.W., Manghnani, M.H., Rai, C.S., Fryer, P. and Ramananantoandro, R., 1976. Elastic properties of selected ophiolite rocks from Papua, New Guinea: Nature and composition of oceanic lower crust and upper mantle. In: G. H. Sutton, M.H. Manghnani and R. Moberly (Editors), The Geophysics of the Pacific Ocean Basin and its Margins. Am. Geophys. Union, Monogr., 19: 407–421.

Kröner, A., 1981. Precambrian plate tectonics. In: A. Kröner (Editor), Precambrian Plate Tectonics. Elsevier, Amsterdam, pp. 57–90.

Kröner, A., 1984. Evolution, growth and stabilization of the Precambrian lithosphere. Phys. Chem. Earth, 15: 69–106.

Lachenbruch, A.H. and Sass, J.H., 1978. Models of an extending lithosphere and heat flow in the Basin and Range province. In: R. B. Smith and G.P. Eaton (Editors), Cenozoic Tectonics and Regional Geophysics of the Western

Cordillera. Geol. Soc. Am., Mem., 152: 209–250.

LASE, S.G., 1986. Deep structure of the U.S. East Coast passive margin from large aperture seismic experimen (LASE). Mar. Pet. Geol., 3: 234–242.

Leaver, D.S., Mooney, W.D. and Kohler, W.M., 1984. A seismic refraction study of the Oregon Cascades. Geophys. Res., 89: 3121–3134.

Litak, R.K. and Brown, L.D., 1989. A modern perspective on the Conrad discontinuity. EOS, Trans. AGU, 70, 713

Lowe, C. and Jacob, A.W.B., 1989. A north–south seismic profile across the Caledonian suture zone in Irelan Tectonophysics, 168: 297–318.

Luetgert, J.H. and C.E., Mann,, 1990. Avalon terrane in eastern coastal Maine: Seismic refraction–wide-ang reflection data. Geology, 18: 878–881.

Luetgert, J.H., Mann, C.E. and Klemperer, S.L., 1987. Wide-angle deep crustal reflections in the norther Appalachians. Geophys. J. R. Astron. Soc., 89: 183–188.

Luosto, U. and Korhonen, H., 1986. Crustal structure of the Baltic Shield along the SVEKA profile in Finland. An Geophys., 5: 639–650.

Luosto, U., Flüh, E.R., Lund, C.-E. and Working Group, 1989. The crustal structure along the POLAR Profile fro seismic refraction investigations. Tectonophysics, 162: 51–85.

Luosto, U., Tiira, T., Korhonen, H., Azbel, I., Burmin, V., Buyanov, A., Kosminskaya, I., Ionkis, V. and Sharo N., 1990. Crust and upper mantle structure along the DSS Baltic profile in SE Finland. Geophys. J. Int., 101 89–110.

Lutter, W.J. and Nowack, R.L., 1990. Inversion for crustal structure using reflections from the PASSCAL Ouachit experiment. J. Geophys. Res., 95: 4633–4646.

MacGregor-Scott, N. and Walter, A., 1988. Crustal velocities near Coalinga, California, modeled from a combine earthquake/explosion refraction profile. Bull. Seismol. Soc. Am., 78: 1475–1490.

Manghnani, M.H., Ramananantoandro, R. and Clark, S.P. Jr., 1974. Compressional and shear wave velocities i granulite facies rocks and eclogites to 10 kilobars. J. Geophys. Res., 79: 5427–5446.

Matthews, D.H. and Cheadle, M.J., 1986. Deep reflections from the Caledonides and Variscides west of Britai and comparison with the Himalayas. In: M. Barazangi and L. Brown (Editors), Reflection Seismology: A Glob Perspective. American Geophysical Union, Geodynamics Series 13, Washington, D.C., pp. 5–19.

Matthews, D.H. and Smith, C., 1987. Deep seismic reflection profiling of the continental lithosphere. Geophys. J R. Astron. Society 89, 498 pp.

McCamy, K., Meyer, R.P. and Smith, T.J., 1962. Generally applicable solutions of Zoeppritz' amplitude equation Bull. Seismol. Soc. Am., 52: 923–955.

McCarthy, J. and Thompson, G.A., 1988. Seismic imaging of extended crust with emphasis on the western Unite States. Geol. Soc. Am. Bull., 100: 1361–1374.

McCarthy, J., et al., 1989. Unpublished PACE results.

McLennan, S.M. and Taylor, S.R., 1982. Geochemical constraints on the growth of the continental crust. J. Geol. 90: 347–361.

McMechan, G.A. and Mooney, W.D., 1980. Asymptotic ray theory and synthetic seismograms for laterally varyin structures: Theory and application to the Imperial Valley, California. Bull. Seismol. Soc. Am., 70: 2021–2035.

Mechie, J., Prodehl, C. and Koptschalitsch, G., 1986. Ray path interpretation of the crustal structure beneath Saud Arabia. Tectonophysics, 131: 333–352.

Meissner, R., 1973. The 'Moho' as a transition zone. Geophys. Surv., 1: 195–216.

Meissner, R., 1986. The Continental Crust, a Geophysical Approach. Academic Press, Orlando, Fla., 426 pp.

Mereu, R.F. and 11 others, 1986. The 1982 COCRUST experiment across the Ottawa–Bonnechere graben an Grenville Front in Ontario and Quebec. Geophys. J. R. Astron. Soc., 84: 491–514.

Mohorovičić, A., 1910. Das Beben vom 8.X.1909. Jahrb. Meteorol. Obs. Zagreb, 9: Teil 4, Abschn. 1.63.

Mooney, W.D., 1989. Seismic methods for determining earthquake source parameters and lithospheric structure. In L.C. Pakiser and W.D. Mooney (Editors), The Geophysical Framework of the Continental United States. Geol Soc. Am., Mem., 172: 11–34.

Mooney, W.D. and Brocher, T.M., 1987. Coincident seismic reflection/refraction studies of the continental litho sphere: a global review. Rev. Geophys., 25: 723–742.

Mooney, W.D. and Prodehl, C., 1978. Crustal structure of the Rhenish Massif and adjacent areas; a reinterpretatio of existing seismic-refraction data. J. Geophys., 44: 573–601.

Mooney, W.D. and Prodehl, C. (Editors), 1984. Proceedings of the 1980 workshop of the International Association of Seismology and Physics of the Earth's Interior on the seismic modeling of laterally varying structures: Contributions based on data from the 1978 Saudi Arabian refraction profile. U.S. Geol. Surv., Circ. 937, 158 pp.

Mooney, W.D., Andrews, M.C., Ginzburg, A., Peters, D.A. and Hamilton, R.M., 1983. Crustal structure of the northern Mississippi embayment and a comparison with other continental rift zones. Tectonophysics, 94: 327–348.

Mooney, W.D., Gettings, M.E., Blank, H.R. and Healy, J.H., 1985. Saudi Arabian seismic refraction profile: a traveltime interpretation of crustal and upper mantle structure. Tectonophysics, 111: 173–246.

Morel-á-l'Huissier, P., Green, A.G. and Pike, C.J., 1987. Crustal refraction surveys across the Trans-Hudson orogen/Williston Basin of South Central Canada. J. Geophys. Res., 92: 6403–6420.

Müller, S., Prodehl, C., Mendes, A.S. and Sousa Moreira, V., 1973. Crustal structure in the southwestern part of the Iberian Peninsula. Tectonophysics, 20: 307–318.

Mykkeltveit, S., 1980. A seismic profile in southern Norway. Pure Appl. Geophys., 118: 1310–1325.

Nur, A. and Simmons, G., 1969. The effect of saturation on velocity in low porosity rocks. Earth Planet. Sci. Lett., 7: 183–193.

Pakiser, L.C. and Brune, J.N., 1980. Seismic models of the root of the Sierra Nevada. Science, 210: 1088–1094.

Pavlenkova, N.I., 1979. Generalized geophysical model and dynamic properties of the continental crust. Tectonophysics, 59: 381–390.

Phinney, R.A. and Roy-Chowdury, K., 1989. Reflection seismic studies of crustal structure in the eastern United States. In: L. C. Pakiser and W.D. Mooney (Editors), The Geophysical Framework of the Continental United States. Geol. Soc. Am., Mem., 172: 613–654.

Powell, C.M.R. and Sinha, M.C., 1987. The PUMA experiment west of Lewis. Geophys. J. R. Astron. Soc., 89: 259–264.

Prodehl, C., Schlittenhardt, J. and Stewart, S.W., 1984. Crustal structure of the Appalachian Highlands in Tennessee. Tectonophysics, 109: 61–76.

Raitt, R.W., Shor, G.G., Jr., Francis, T.J.G. and Morris, G.B., 1969. Anisotropy of the Pacific upper mantle. J. Geophys. Res., 74: 3095–3109.

Reiter, E.C., Purdy, G.M., Sawyer, D., Stoffa, P.L., Phillips, J.A., Austin, J.A., Jr. and Toksoz, N., 1988. Ocean bottom hydrophone results from a multichannel seismic survey in the Carolina Trough and Southeast Georgia Embayment [abs.]. EOS, Trans. AGU 69: 1405.

Research Group for Seismology, 1973. Crustal structure of Japan as derived from explosion seismic data. Tectonophysics, 20: 129–135.

Reymer, A. and Schubert, G., 1984. Phanerozoic addition rates to the continental crust and crustal growth. Tectonics, 3: 63–77.

Rudnick, R.L. and Taylor, S.R., 1986. Geochemical constraints on the origin of Archean tonalitic-trondhjemtic rocks and implications for lower crustal composition. In: J. B. Dawson, D.A. Carswell, J. Hall and K.H. Wedepohl (Editors), The Nature of the Lower Continental Crust. Geol. Soc. London, Geol. Soc. Spec. Publ., 24: 179–191.

Sapin, M., Wang, X.-J., Hirn, A. and Z.X., Xu,, 1985. A seismic sounding in the crust of the Lhasa block, Tibet. Ann. Geophys., 3: 637–646.

Schock, R.N., Bonner, B.P. and Louis, H., 1974. Collection of ultrasonic velocity data as a function of pressure for polycrystalline solids. National Tech. Info. Servide, Lawrence Livermore Lab. Tech. Rept., UCRL-51508 Springfield, Va., 262 pp.

Shankland, T.J. and Ander, M.E., 1983. Electrical conductivity, temperatures and fluids in the lower crust. J. Geophys. Res., 88: 9475–9484.

Shaw, D.M., Cramer, J.J., Higgins, M.D. and Truscott, M.G., 1986. Composition of the Canadian Precambrian shield and the continental crust of the earth. In: J. B. Dawson, D.A. Carswell, J. Hall and K.H. Wedepohl (Editors), The Nature of the Lower Continental Crust. Geol. Soc. London, Geol. Soc. Spec. Publ., 24: 275–282.

Simmons, G., 1964. Velocity of shear waves in rocks to 10 kilobars. J. Geophys. Res., 69: 1123–1130.

Simmons, G. and Brace, W.F., 1965. Comparison of static and dynamic measurements of compressibility of rocks. J. Geophys. Res., 70: 5649–5656.

Sinno, Y.A., Daggett, P.H., Keller, G.R., Morgan, P. and Harder, S.H., 1986. Crustal structure of the southern Rio Grande Rift determined from seismic refraction profiling. J. Geophys. Res., 91: 6143–6156.

Sleep, N.H. and Windley, B.F., 1982. Archean plate tectonics: Constraints and inferences. J. Geol., 90: 363–379.

Smithson, S.B., 1978. Modeling continental crust: structural and chemical constraints. Geophys. Res. Lett., 5: 749–752.

Smithson, S.B., 1986. A physical model of the lower crust from North America based on seismic reflection data. In: J. B. Dawson (Editor), The Nature of the Lower Continental Crust. Geol. Soc. London, Geol. Soc. Spec. Publ., 25: 23–34.

Smithson, S.B. and Brown, S.K., 1977. A model for lower continental crust. Earth Planet. Sci. Lett., 35: 134–144.

Smithson, S.B. and Johnson, R., 1989. Crustal structure of the western U.S. based on reflection seismology. In: L. C. Pakiser and W.D. Mooney (Editors), Geophysical Framework of the Continental United States. Geol. Soc. Am., Mem., 172: 577–612.

Smithson, S.B., Johnson, R.A. and Wong, Y.K., 1981. Mean crustal velocity: a critical parameter for interpreting crustal structure and crustal growth. Earth Planet. Sci. Lett., 53: 323–332.

Sollogub, V.B., Litvinenko, I.V., Chekunov, A.V., Ankudinov, S.A., Ivanov, A.A., Kalyuzhnaya, L.T., Kokorina, L.K. and Tripolsky, A.A., 1973. New D.S.S. data on the crustal structure of the Baltic and Ukrainian shields. Tectonophysics, 20: 67–84.

Sparlin, M.A., Braile, L.W. and Smith, R.B., 1982. Crustal structure of the eastern Snake River Plain determined from ray trace modeling of seismic refraction data. J. Geophys, Res., 87: 2619–2633.

Stauber, D.A., 1983. Crustal structure in northern Nevada from seismic refraction data. In: Geothermal Resources Council, Spec. Rep., 13: 319–332.

Stoffa, P.L. and Buhl, P., 1979. Two-ship multichannel seismic experiments for deep crustal studies: Expanded spread and constant offset profiles. J. Geophys. Res., 84: 7645–7660.

Tarkov, A.P., Basula, I.P., Generalov, V.G., Dubyansky, A.I. and Chernykh, V.V., 1981. Composite travel times of seismic waves and general velocity models of the Voronezh Shield crust and upper mantle. Geophys. J. R. Astron. Soc., 67: 137–143.

Tarney, J. and Windley, B.F., 1977. Chemistry, thermal gradients and evolution of the lower continental crust. J. Geol. Soc. London, 134: 153–172.

Taylor, S.R., 1977. Island arc models and the composition of the continental crust. In: M. Talwani and W.C. Pitman (Editors), Am. Geophys. Union, Maurice Ewing Series, 1: 229–242.

Taylor, S.R. and McLennan, S.M., 1981. The composition and evolution of the continental crust: rare earth element evidence from sedimentary rocks. Philos. Trans. R. Soc. London, 301: 381–399.

Teng, J., Xiong, S., Yin, Z., Xu, Z., Wang, X. and Lu, D., 1985. Structure of the crust and upper mantle pattern and velocity distributional characteristics in the northern Himalayan mountain region. J. Phys. Earth, 33: 157–171.

Todd, T. and Simmons, G., 1972. Effect of pore pressure on the velocity of compressional waves in low-porosity rocks. J. Geophys. Res., 77: 3731–3743.

Trehu, A.M. and Wheeler, W.H., IV, 1987. Possible evidence for subducted sedimentary materials beneath central California. Geology, 15: 254–258.

Trehu, A.M., Ballard, A., Dorman, L.M., Gettrust, J.F., Klitgord, K.D. and Schreiner, A., 1989. Structure of the lower crust beneath the Carolina Trough, U.S. Atlantic continental margin. J. Geophys. Res., 94: 10,585–10,600.

Wang, H., Todd, T., Richter, D. and Simmons, G., 1973. Elastic properties of plagioclase aggregates and seismic velocities in the moon. Proc. 4th Lunar Sci. Conf., 4-3: 2663–2671.

Weaver, B.L. and Tarney, J., 1984. Empirical approach to estimating the composition of the continental crust. Nature, 310: 575–577.

Wever, T., 1989. The Conrad discontinuity and the top of the reflective lower crust –do they coincide? Tectonophysics, 157: 39–58.

White, R.S., Spence, G.D., Fowler, S.R., McKenzie, D.P., Westbrook, G.K. and Bowen, A.N., 1987. Magmatism at rifted continental margins. Nature, 330: 439–444.

White, R.S. and McKenzie, D., 1989. Magmatism at rift zones: The generation of volcanic continental margins and flood basalts. J. Geophys. Res., 94: 7685–7730.

Windley, B.F., 1981. Precambrian rocks in the light of the plate-tectonic concept. In: A. Kröner (Editor), Precambrian Plate Tectonics. Elsevier, Amsterdam, pp. 1–20.

Wilson, J.M., McCarthy, J., Johnson, R.A. and Howard, K.A., 1991. An axial view of a metamorphic core complex: Structure of the Whipple and Chemehuevi Mountains, southeastern California. J. Geophys. Res., 96: 12,293–12,311.

Yan, Q.Z. and Mechie, J., 1989. A fine structural section through the crust and lower lithosphere along the axial region of the Alps. Geophys. J., 98: 465–488.

Yuan, X., Wang, S., Li, L. and Zhu, J., 1986. A geophysical investigation of deep structure in China. In: M. Barazangi and L. Brown (Editors), Reflection Seismology: A Global Perspective. American Geophysical Union, Geodynamics Series 13, Washington, D.C., pp. 151–160.

Zandt, G. and Owens, T.J., 1986. Comparison of crustal velocity profiles determined by seismic refraction and teleseismic methods. Tectonophysics, 128: 155–161.

Zeis, S., Gajewski, D. and Prodehl, C., 1990. Crustal structure of southern Germany from seismic refraction data. Tectonophysics, 176: 59–86.

Zelt, C.A. and Ellis, R.M., 1989. Seismic structure of the crust and upper mantle in the Peace River Arch region, Canada. J. Geophys. Res., 94: 5729–5744.

Zucca, J.J., 1984. The crustal structure of the southern Rhinegraben from re-interpretation of seismic refraction data. J. Geophys., 55: 13–22.